Studies on infection-promoting effectors in plant growth-promoting fungi

Hong Ye
Nara Institute of Science and Technology
Graduate School of Biological Sciences
Laboratory of Plant Immunity
Yusuke Saijo
Submission date 2021/07/26

Laboratory (Supervisor)	Laboratory of Plant Immunity (Prof. Yusuke Saijo)		
Name	Hong Ye	Date	07, 26, 2021
Title	Studies on infection-promoting effectors in plant growth-promoting fungi		

ABSTRACT

Plants naturally accommodate a diversity microorganisms ranging from beneficial endophytes to harmful pathogens. Beneficial endophytes provide the host with fitness benefits such as biotic/abiotic stress tolerance or plant growth promotion (PGP). In contrast, pathogen infection causes detrimental effects that result in plant diseases. Notably, otherwise mutualistic microbes can also negatively influence plant health, depending on the environmental conditions and/or host genetic backgrounds. This indicates the existence of virulence mechanisms in mutualistic microbes, and also their suppression as a key step in beneficial interactions. However, the mechanisms by which mutualistic microbes infect the host, with or without expressing potential virulence, remain poorly understood compared to pathogens.

The genus *Colletotrichum* represents a large group of phytopathogens causing anthracnose diseases on a diverse range of economically important crops as well as the model plant *Arabidopsis thaliana*. A root fungal endophyte *Colletotrichum tofieldiae* (*Ct*) promotes plant growth in *A. thaliana* under phosphate limiting conditions via transferring phosphorus to the hosts. In Brassicaceae, tryptophan (Trp)-derived secondary metabolites such as camalexin and indole glucosinolates play critical roles in restricting growth of both pathogenic and beneficial microbes. In *cyp79B2 cyp79B3* plants devoid of Trp-derived secondary metabolites, *Ct* overgrows and turns to be a pathogen, suggesting a critical role for metabolite-based fungal growth control in beneficial interactions with *Ct*. Little is known, however, about the mechanisms by which *Ct* overgrowth and pathogenesis are prevented in the presence of Trp-derived plant metabolites, or otherwise *Ct* displays pathogenesis in their absence.

I first examined the possible involvement of different Trp-derived metabolites in suppression of *Ct* overgrowth, by directly applying synthesized metabolites to *A. thaliana* during *Ct* colonization. *Ct* overgrowth in *cyp79B2 cyp79B3* was specifically attenuated with exogenous application of camalexin and 4-methoxyindol-3-ylmethyl amine (4MI3A). Interestingly, 4MI3A, an as-yet-uncharacterized indole glucosinolate-related metabolite, inhibits fungal growth specifically *in planta* but not in culture, suggesting that 4MI3A and/or its derivatives effectively suppress *Ct* growth specifically within the host tissues.

Pathogenic and beneficial microbes employ secreted effector proteins to promote host infection. To investigate whether *Ct* has infection-promoting effectors and if so how they

contribute to *Ct* infection, or whether they are suppressed during beneficial interactions by the aforementioned host metabolites, we put a particular focus on candidate secreted effector proteins (CSEPs) that are de-repressed in *cyp79B2 cyp79B3* plants. Transcriptome analysis of *Ct*-inoculated plants revealed 11 *CSEP* genes in *Ct*, which are silenced in the wild type (WT) but up-regulated in *cyp79B2 cyp79B3* plants. To assess possible roles for these *CSEPs* in *Ct* root colonization, I determined *Ct* fungal biomass in transgenic *A. thaliana* plants constitutively expressing individual *CSEPs*. Of them, introduction of *CSEP2* and *CSEP9*, without the signal peptide sequences permitted enhanced *Ct* growth, providing evidence that *CSEP2* and *CSEP9* contribute to *Ct* infection in roots. *CSEP2* orthologues are conserved across diverse *Colletotrichum* species, while in contrast *CSEP9* seems to be specific to *Ct*. The results suggest that *CSEP2* is likely to play a common role as an infection-promoting factor in the *Colletotrichum* genus. Notably, *in planta* overexpression of *CSEP2* significantly impaired callose deposition in response to microbe-associated molecular patterns (MAMPs), elicitor-active structures typical of microbes, suggesting that *CSEP2* serves to suppress MAMP-induced cell wall defense.

It has been reported that the Trp-derived indole glucosinolate pathway is also required for MAMP-induced callose deposition in *A. thaliana*. I thus tested the possible relationship between *CSEP2* and the host indole glucosinolate pathway in *CSEP2* suppression of MAMP-induced callose deposition. Exogenous application of 4MI3A, a predicted indole glucosinolate hydrolytic product, rescued MAMP-induced callose deposition in *CSEP2*-expressing plants, whereas Indole-3-ylmethyl-glucosinolate (I3G), produced upstream of 4MI3A, did not. The results imply that the reinforcement of indole glucosinolate metabolism can counteract *CSEP2*-mediated callose suppression, and that *CSEP2* interferes with some step upstream of 4MI3A but downstream of I3G in the indole glucosinolate pathway. Consistently, in *pmr4* lacking the callose synthase responsible for defense-associated callose deposition, *Ct* growth was increased compared to WT. This suggests that *Ct* colonization is restricted by *PMR4*-mediated callose deposition, and that *Ct* can counteract the cell wall-based defense with *CSEP2*.

In summary, my study successfully reveals an endophytic fungal effector, *CSEP2*, which is silenced during beneficial interactions but can attenuate a cell wall-based defense to promote fungal infection. The results also suggest *CSEP2* suppression with the host Trp-derived metabolites as a critical step in preventing overgrowth and pathogenesis of endophytic fungi. This seems to be achieved at both the levels of the effector expression and functioning. Furthermore, this study indicates 4MI3A application as an effective means to control *Ct* growth for obtaining its benefits. This work illuminates an important balance between a fungal effector and host Trp-derived metabolites, over MAMP-induced callose deposition, which controls the outcome of plant interactions with beneficial endophytic fungi.

Table of Contents

ABBREVIATIONS

1MI3A	1-Methoxyindol-3-ylmethylamine
1MI3G	1-Methoxyindol-3-ylmethyl glucosinolate
1OHI3G	1-Hydroxy-indole-3-ylmethyl glucosinolate
4MI3A	4-Methoxyindol-3-ylmethylamine
4MI3G	4-Methoxyindol-3-ylmethyl glucosinolate
4OHI3G	4-Hydroxy-indole-3-ylmethyl glucosinolate
4OHICN	4-Hydroxyindole-3-carbonyl nitrile
AA	Amino acids
AMF	*Arbuscular mycorrhizal fungi*
CAM	Camalexin
CDPK	Calcium-dependent protein kinases
CERK	CHITIN ELICITOR RECEPTOR KINASE
Ci	*Colletotrichum incanum*
CSEPs	Candidate secreted effector proteins
Ct	*Colletotrichum tofieldiae*
CYP79B2	*CYTOCHROME P450, FAMILY 79, SUBFAMILY B, POLYPEPTIDE 2*
CYP79B3	*CYTOCHROME P450, FAMILY 79, SUBFAMILY B, POLYPEPTIDE 3*
Cys	Cysteine
DMSO	Dimethyl Sulfoxide
dpi	Days post inoculation
ET	Ethylene
ETI	Effector-triggered immunity
EWCAs	Effectors with chitinase activity
FLS2	*FLAGELLIN-SENSITIVE 2*
hpi	Hours post inoculation
I3A	Indol-3-ylmethylamine
I3C	Indole-3-carbinol
I3G	Indole-3-ylmethyl-glucosinolate
IAA	Indole-3-acetic acid
IAN	Indole-3-acetonitrile
IAOx	Indole-3-acetaldoxime
ICA	Indole-3-carboxylic acid
ICN	Indole-3-carbonyl nitrile
IGs	Indole-glucosinolate derivatives
JA	Jasmonic Acid
LC/MS	Liquid chromatography-mass spectrometry

LRR	Leucine-Rich Repeat
LYK5	Lysin motif receptor kinase 5
MAMPs	Microbe-Associated Molecular Patterns
MAPK	Mitogen-activated protein kinase
MS	Murashige and Skoog medium
PAD3	*PHYTOALEXIN DEFICIENT 3*
PAMPs	Pathogen-Associated Molecular Patterns
PCR	Polymerase Chain Reaction
PEN2	*PENETRATION2*
PGP	Plant Growth Promotion
PMR4	*POWDERY MILDEW RESISTANT 4*
PGNs	Peptidoglycans
PRRs	Pattern Recognition Receptors
PTI	Pattern-triggered immunity
qRT-PCR	Quantitative Reverse Transcription Polymerase Chain reaction
RA	Raphanusamic acid
RLKs	Receptor Like Kinases
ROS	Reactive Oxygen Species
SA	Salicylic Acid
SID2	*SALICYLIC ACID INDUCTION DEFICIENT 2*
SP	Signal Peptide
Trp	Tryptophan

INTRODUCTION

Plant-microbe interactions range from beneficial to pathogenic modes

Plants are continually exposed to a vast diversity of microbes ranging from beneficial endophytes to harmful pathogens. Plants interact with beneficial microbes in a synergistic way or interact with pathogens in an antagonistic manner (Binyamin et al., 2019). From commensal to mutualistic or pathogenic relationships between plants and microbes are influenced by plant immune responses, including antimicrobial metabolites and phytohormones, and also by environmental parameters (Hacquard et al., 2017). Bacteria and fungi that colonize living plant tissues without causing apparent disease symptoms, at least during parts of their life-styles, are called endophytes. By contrast, microbes that cause diseases are called pathogens. Importantly, however, endophytes and pathogens cannot be seen as static dichotomy. It has been well documented that infectious microbes dynamically change their lifestyles depending on the surrounding environments. For example, *B. amyloliquefaciens* GB03 is a plant growth-promoting rhizobacterium under phosphate-sufficient conditions, but turns to be a pathogen under phosphate-deficient conditions (Morcillo et al., 2020).

Under abiotic stress conditions, especially under limited nutrition, some endophytes show plant growth promotion (PGP) effects (Hiruma et al., 2018). Inorganic phosphate (Pi) limitation often occurs in soil and profoundly constrains plant growth. In fact, in over 60% of global arable land, low-phosphate availability limits crop yield (Lynch, 2011). Pi-solubilizing microbes increase soil phosphorus availability for the plant by mobilizing insoluble phosphate into soluble, plant-accessible phosphate (Antoun, 2012). Arbuscular mycorrhizal fungi (AMF) are among the best-documented beneficial fungi colonizing more than 70% of land plant species. AMF absorb and supply soil nutrients to plants, thereby increasing in particular Pi uptake efficiency to promote plant growth, but do not colonize *Brassicaceae* plants, including *Arabidopsis thaliana* (Bonfante and Genre, 2010; Habte, 2006; Manjunath et al, 1989; Vosatka and Albrechtova, 2009). *Colletotrichum tofieldiae* (*Ct*) colonizes *Arabidopsis thaliana* roots to mobilize insoluble soil phosphate such as calcium phosphate to bioavailable Pi, and thereby transfers this macronutrient phosphorus to the host specifically under Pi-deficient conditions. By contrast, *Ct* does not show PGP in Pi-replete conditions, suggesting that *Ct* beneficial effects are phosphate status dependent (Hiruma et al., 2016). By contrast, *Colletotrichum incanum* (*Ci*), a close pathogenic relative of *Ct*, does not translocate enough Pi into the host plant for growth promotion, and causes plant necrosis (Hacquard et al., 2016; Hiruma et al., 2016).

A large number of plant metabolites have roles in pathogen resistance (Rojas et al., 2014; Zaynab et al., 2018). For example, the aliphatic glucosinolate derivative sulforaphane covalently modifies the 209th Cys (Cys209) of HrpS, one of the major components of

bacterial Type III secretion system (T3SS) to inhibit *Psedomonas syringae* virulence effector delivery to plants (Wang et al., 2020). Plant Trp-derived secondary metabolites play a critical role in fungal resistance, and are also required for beneficial interactions between *A. thaliana* and endophytic microbes (Hiruma et al., 2016; Lahrmann et al., 2015; Nongbri et al., 2012). *A. thaliana* mutant *cyp79B2 cyp79B3*, disrupted with an initial rate-limiting step in Trp-derived metabolic pathways, fails to prevent overgrowth and pathogenesis of *Ct* (Hiruma et al., 2016). *Ct* also excessively colonizes *A. thaliana* relatives *Capsella rubella*, which inherently lacks indole glucosinolates, to strongly inhibit plant growth (Bednarek et al., 2011; Hiruma et al., 2016). However, what in *Ct* promotes fungal infection in the absence of host Trp metabolism and what is suppressed in its presence, and their functional significance remain largely unknown.

Plant Trp-derived secondary metabolites in plant defense

To adapt to different abiotic and biotic stresses in nature, plants have evolved intricate mechanisms including involving a wide array of secondary metabolites, thereby thriving in a given ecological niche (Dixon, 2001). *Brassicaceae* plant species are characterized by a multitude of secondary metabolites, including terpenes, phenolics, alkaloids and glycosides, promoting their stress adaptation. In particular, Trp-derived secondary metabolites play critical roles in plant defense against pathogenic microorganisms and pests (Hiruma et al., 2013).

Two redundant Arabidopsis cytochrome P450s, *CYP79B2* and *CYP79B3*, which convert Trp to indole-3-acetaldoxime (IAOx), an important intermediate of Trp-derived secondary metabolites, are critical for Trp metabolism associated with biotic stress adaptation (Zhao et al., 2002; Bohinc et al., 2012; Hiruma., 2019) (Figure 1). Downstream of IAOx, different metabolic branches mediate biosynthesis of indole glucosinolate (IG), the indolic phytoalexin camalexin, indole-3-carboxylic acid (ICA), indole-3-carbonyl nitrile (ICN) and indole-3-acetic acid (IAA), which have been implicated in immune responses (Glawischnig et al., 2004; Hagemeier et al., 2001; Pastorczyk and Bednarek, 2016; Pastorczyk et al., 2020; Rajniak et al., 2015) (Figure 1B). Genetic studies have revealed that the IG and camalexin pathways contribute to antifungal defense (Hiruma et al., 2010; Schlaeppi et al., 2010). Camalexin is synthesized via indole-3-acetonitrile (IAN) downstream of IAOx (Glawischnig et al., 2004). The cytochrome P450 monooxygenase, *CYP71B15* (*PAD3*), catalyzes the biosynthesis of camalexin, and plays a critical role in pathogen resistance (Glawischnig, 2007; Schuhegger et al., 2006; Zhou et al., 1999). Two *CYP71A12* and *CYP71A13* monooxygenases are responsible for ICA biosynthesis, and contribute to resistance against pathogens of two different lifestyles, *Plectosphaerella cucumerina* and *Colletotrichum tropicale* (Pastorczyk et al., 2020). A pathogen-induced cytochrome P450, *CYF82C2*, mediates the conversion from ICN to 4-hydroxyindole-3-carbonyl nitrile (4OHICN), and plays a crucial role in plant

defense against bacterial pathogen *Pseudomonas syringae* (Rajniak et al., 2015). Indole-3-carbinol (I3C) is a breakdown product from indole-3-ylmethyl-glucosinolate (I3G) in crucifer species and involved in plant defense (Agerbirk et al., 2009; Clay et al., 2009; Fahey et al., 2001) (Figure 1).

The gene subfamilies of cytochrome P450 monooxygenases, CYP81Fs, have the biochemical capacity to modify Indole-3-ylmethyl-glucosinolate (I3G) to produce partially overlapping spectra of metabolites. *CYP81F4* catalyzes the conversion of I3G to 1-methoxyindol-3-ylmethyl glucosinolate (1MI3G), whereas an unstable intermediate 1-hydroxy-indole-3-ylmethyl glucosinolate (1OHI3G) has not been reported yet (Pfalz et al., 2011). *CYP81F2* and *CYP81F3* are responsible for the hydroxylation of I3G to 4-hydroxy-indole-3-ylmethyl glucosinolate (4OHI3G), which is essential for the pathogen-induced accumulation of 4-methoxyindol-3-ylmethyl glucosinolate (4MI3G) (Bednarek et al., 2009; Pfalz et al., 2009; Pfalz et al., 2011). 4MI3G is activated by the atypical PEN2 myrosinase for antifungal defense. PEN2 glycosyl hydrolase is localized to the peroxisomes, and participates in inducible pre-invasion resistance (Lipka et al., 2005). 4MI3G is a biologically relevant substrate of PEN2 and cleavage of 4MI3G is essential for plant defense (Bednarek et al., 2009). 4-Methoxyindol-3-ylmethylamine (4MI3A), a predicted product derived from 4MI3G by PEN2, has not been detected *in planta* by liquid chromatography-mass spectrometry (LC/MS) (Bednarek et al., 2009) (Figure 1).

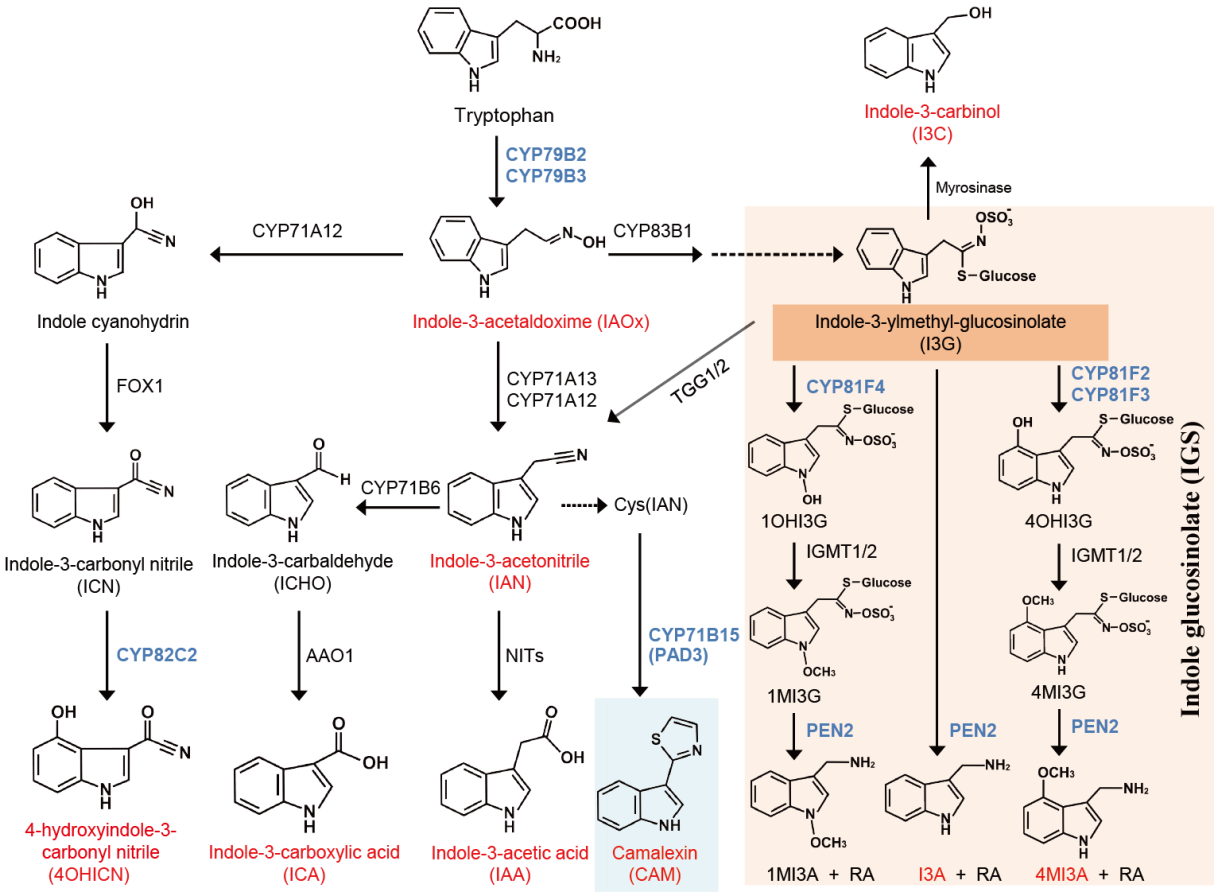

Figure 1. A scheme for Trp-derived secondary metabolism in *A. thaliana*.
The enzymes discussed in this study are highlighted by blue. Key intermediates and breakdown products used in this study are highlighted in red. The indole glucosinolate (IG) and camalexin pathways are shadowed in orange and green, respectively. RA, raphanusamic acid.

Plant defenses and effectors

Plants have evolved a multilayered immune system to halt pathogen growth and disease. A first layer of plant innate immunity is generally initiated upon perception of pathogen-associated molecular patterns (PAMPs) or microbe-associated molecular patterns (MAMPs) (Cook et al., 2015), such as bacterial flagellin, fungal oligosaccharide chitin, lipopolysaccharides, and peptidoglycans (PGNs) (Boller et al., 2009; Saijo et al., 2018). These PAMPs/MAMPs are perceived by pattern recognition receptors (PRRs) at cell surfaces, thereby, leading to an enhanced state of immunity, termed pattern-triggered immunity (PTI). An *N*-terminal 22-amino-acid epitope of flagellin, flg22, is perceived by the leucine-rich repeat (LRR) domains of the receptor-like kinase FLAGELLIN-SENSING 2 (FLS2) in plants (Felix et al., 1999; Gómez et al., 2000; Millet et al., 2010). Fungal chitin, a sugar polymer of *N*-acetylglucosamine which is a major component of the fungal cell wall, triggers immune responses (Millet et al., 2010), upon perception by the lysin motif receptor kinase 5 (LYK5)

and co-receptor CERK1 in *A. thaliana* (Miya et al., 2007; Shinya et al., 2015). Pathogens produce and secrete effector proteins to inhibit host PTI. Plants typically detect effectors with an additional class of cytoplasmic-resident receptors, predominantly nucleotide-binding LRR receptors (NB-LRR), to activate a potent form of plant immunity termed effector-triggered immunity (ETI) (Boller et al, 2009; Jones et al, 2006) (Figure 2A).

PRR-mediated MAMP recognition triggers an array of defense responses, including Ca^{2+}- and reactive oxygen species (ROS)-bursts, ethylene production, mitogen-activated protein kinase (MAPK) cascade activation and extensive reprogramming of transcriptome, proteome and metabolome. MAMP recognition also triggers biosynthesis of callose, high-molecular-weight β (1-3)-glucan polymers, which are frequently deposited in the cell wall appositions (papillae) at the site of pathogen contact to provide a physical barrier to pathogen invasion (Aist, 1976; Aist and Bushnell, 1991; Meyer et al., 2009; Millet et al., 2010; Nishimura et al., 2003) (Figure 2A and B). Defense-associated callose deposition occurs through the callose synthase *PMR4*, which has been identified as the causative gene mutated in a powdery mildew-resistant *A. thaliana* mutant, called *pmr4* (Vogel et al., 2000). Loss of *PMR4* results in de-repression of SA-based defense and strong pathogen resistance, coincident with a great decrease in callose deposition at the papillae and wounded sites under biotic and abiotic stresses (Nishimura et al., 2003; Vogel et al., 2000). Conversely, overexpression of *PMR4* in *A. thaliana* lowers the penetration rate of powdery mildew fungi (Ellinger et al., 2013), with *PMR4*-dependent callose-rich papillae formed at the sites of pathogen penetration (Aist, 1976; Voigt, 2014). These apparent discrepancies can be explained in a model in which callose deposition defects during PTI are linked to strong activation of SA-dependent backup defense.

Interestingly, the biosynthesis and hydrolysis of IGs are also required for flg22-induced callose deposition under sterile conditions (Clay et al., 2009; Millet et al., 2010). IG biosynthetic and hydrolytic mutants, *cyp79B2 cyp79B3*, *cyp81F2* and *pen2*, show defects in flg22-induced callose deposition in leaves and roots (Clay et al., 2009; Millet et al., 2010). 4MI3G restores callose formation in the IG biosynthetic mutants, whereas it fails to do so in *pen2* (Clay et al., 2009). The metabolites derived from 4MI3G regulating flg22-induced callose deposition remain to be described in the IG pathway.

In co-evolution with the host plants, pathogenic microbes have evolved sophisticated mechanisms to avoid or counteract the host PTI, represented by a wide array of effectors. Pathogenic microbes secrete distinct classes of effector proteins into the apoplasm or cytoplasm of the host to suppress immune responses (Wu et al., 2003; Tintor et al., 2020), thereby promoting pathogen infection. Bacterial effectors, injected predominantly via T3SS, generally target PTI signaling components (Dou et al., 2012; Grant et al., 2006). Fungal effectors also interfere with MAMP perception (Wawra et al., 2016), and repress intracellular PTI signaling as well (Di et al., 2017; Irieda et al., 2019; Tintor et al., 2020). However, the molecular mechanisms by which fungal effectors manipulate their host immunity remain less

understood, compared to bacterial effectors.

Fungal effectors are typically small secreted proteins, most of which have ≤ 300 amino-acid length and carry an *N*-terminal signal peptide (SP, usually 16-30 amino acids) that allows effector secretion from fungal cells (Presti et al., 2015; Schmidt et al., 2013). Moreover, they are typically specific to related fungal species, and orthologous proteins are often absent outside the genus. Most of fungal effectors are Cys rich, a feature that is assumed to enhance effector stability in the host apoplasm (Wang et al., 2020). Although much has been described for pathogen effectors, little is known about host targets and functional roles of effectors in endophytic fungi.

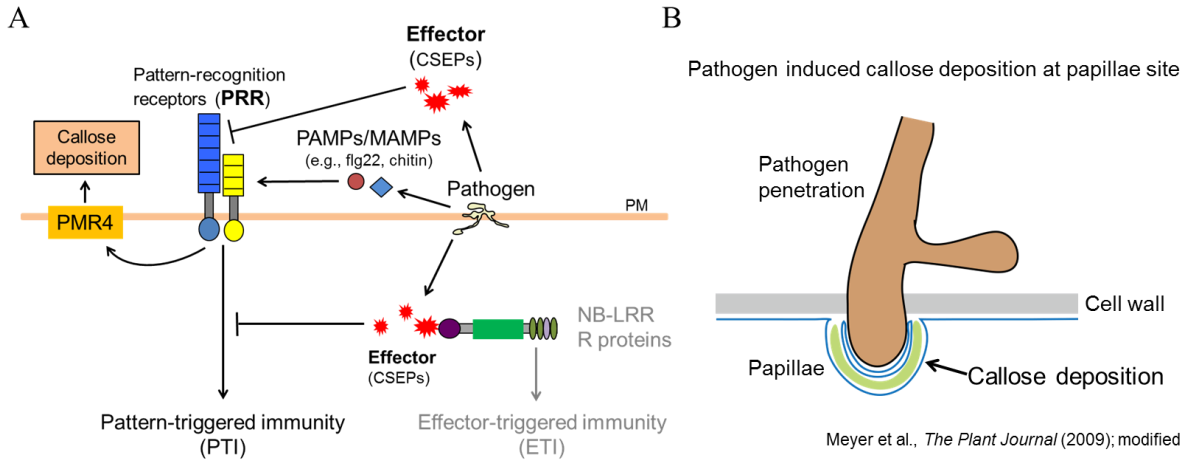

Figure 2. The principles of pathogen triggered plant immunity in *A. thaliana*.
(A) Schematic view of PAMP/MAMP and effector-triggered immunity in plants. Apoplastic pathogen-associated molecular patterns (PAMPs) are perceived by pattern recognition receptors (PRRs) at the cell surface, resulting in the activation of pattern-triggered immunity (PTI). Flagellin (flg22) and chitin have been identified as bacterial and fungal PAMPs, respectively. Pathogens secrete effectors in the apoplast or inject them into the cytoplasm for the suppressing PTI. When cytoplasmic effectors are directly or indirectly recognized by nucleotide-binding LRR receptors (NB-LRR), effector-triggered immunity (ETI) is mounted to terminate pathogen growth. One PTI output involves PMR4 callose synthase to induce callose deposition.
(B) Pathogen-induced callose deposition in the cell wall papillae at pathogen penetration sites increases resistance to pathogen invasion.

Colletotrichum species and Candidate Secreted Effector Proteins (CSEPs)

Colletotrichum is an economically important fungal genus known as pathogenic fungi worldwide, but also includes endophytic species (Jayawardena et al., 2016). The genus comprises more than 189 species geographically distributed throughout the world (Jayawardena et al., 2016; Khodadadi et al., 2020). Many of the species in this genus are

primarily described as pathogens causing anthracnose diseases on a diverse range of economically important crops (Cai et al., 2009; Cannon et al., 2012; Jayawardena et al., 2016). A recent study has described an endophytic *Colletotrichum* fungus, *C. tofieldiae* (*Ct*), which can alter the infection strategies ranging from beneficial to pathogenic in a context-dependent manner (Hiruma et al., 2016). *Ct* has been discovered as an endophyte that grows in the natural population of *A. thaliana* in central Spain. *Ct* can promote plant growth in *A. thaliana* under Pi limiting conditions (Hiruma et al., 2016). *Ct* colonization also improves yield in tomato and maize under optimal nutritional conditions (D áz-Gonz áez et al., 2020). However, its pathogenic relative *C. incanum* (*Ci*), isolated from radish leaves in Japan, can strongly inhibit *A. thaliana* growth and cause diseases following root infection (Hiruma et al., 2016). *Ct* and *Ci* both colonize root epidermal cells in the differentiation zones, but *Ci* infects the host more extensively (Hacquard et al., 2016). Genomes of *Colletotrichum* species have more than 100 genes encoding Candidate Secreted Proteins (CSEPs), defined as extracellular secreted proteins with no significant BLAST similarity (e value < 1×10^{-3}) to sequences outside the genus *Colletotrichum* in the UniProt database (Hacquard et al., 2016). Comparative genomics between *Ct* and *Ci* point out an increased number of CSEPs in *Ci* compared to *Ct* (189 in *Ci* versus 133 in *Ct*). *In-planta* activation of *CSEP* expression is more pronounced in *Ci* (55/189) compared with endophytic *Ct* (18/133) (Figure 3) (Hacquard et al., 2016). This suggests that *CSEP* gene expression is associated with fungal pathogenesis, and that a majority of *CSEPs* are silenced during *Ct* colonization under low Pi conditions. Conceivably, these CSEPs, if expressed, may act as virulence-promoting factors to switch *Ct* lifestyle from the endophytic to pathogenic mode.

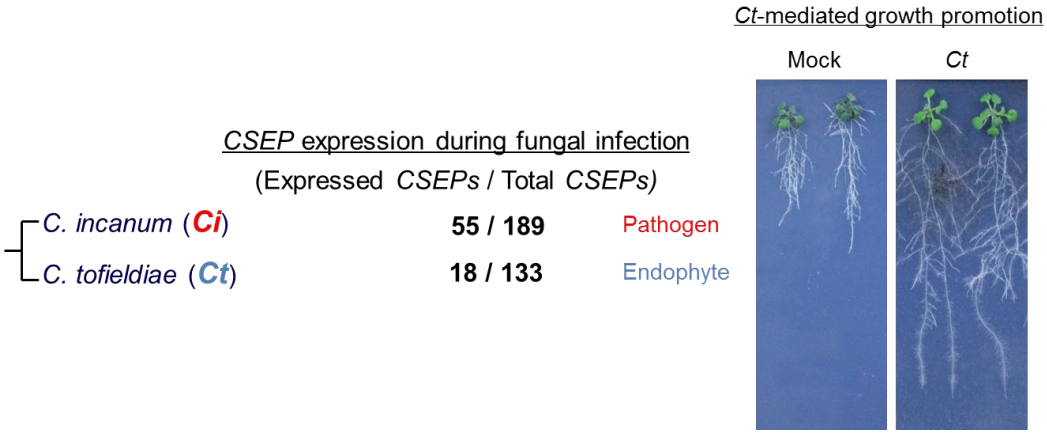

Figure 3. Comparative analysis of lifestyles of endophytic *Ct* and pathogenic *Ci*.
Colletotrichum fungi *Colletotrichum tofieldiae* (*Ct*) is an endophyte, and its closely relative species *C. incanum* (*Ci*) is a pathogen. Endophytic fungus *Ct* can promote Arabidopsis growth under low Pi conditions (50 μM KH_2PO_4). *Ci* has 189 CSEP genes and *Ct* has 133 CSEP genes annotated in the genomes. A greater number of CSEPs are activated in pathogenic *Ci* (55/189) compared with endophytic *Ct* (18/133) during root colonization of WT plants (Hacquard et al., 2016).

Aims of this study

In this study, I aim to examine whether *Ct* endophyte has effectors to promote its infection, and if so, to identify their functional roles and host targets. Moreover, I also aim to elucidate how plant Trp-derived metabolites suppress *Ct* overgrowth and investigate the possible regulation of the identified fungal effector(s) by these metabolites. For this purpose, I pursued the hypothesis that *CSEP* genes in *Ct* suppressed by host Trp-derived metabolites during beneficial interactions have the ability to promote fungal infection, with an assumption that their effects on the host, if expressed, can be readily detectable and amenable to functional studies. I have identified two *Ct CSEPs* that are highly expressed along fungal pathogenesis in *cyp79B2 cyp79B3* mutant plants, and contribute to fungal growth in roots. I have further shown a role for *CSEP2* in suppressing a PTI output, callose deposition. Moreover, I have revealed an as-yet-uncharacterized Trp-derived metabolite, which effectively suppresses the expression of *CSEP* genes and *Ct* overgrowth when applied in *cyp79B2 cyp79B3* mutants. This work provides important insight into the molecular basis for endophytic fungal infection and for the plant control of endophytic fungi toward beneficial interactions.

MATERIALS AND METHODS

Plant materials and growth conditions

The *Arabidopsis thaliana* accession Col-0 was used as the wild type (WT). Seeds were surface sterilized with 6% sodium hypochlorite plus 0.1% Triton X-10 for 15 minutes, and then rinsed with autoclaved distilled water 3 times. The seeds were sown on a half strength Skoog-Murashige (MS) agar medium with 25 mM sucrose. After incubation at 4℃ for 2 days, the plates were placed vertically in a plant growth chamber under 16 h light/ 8 h dark at 22℃. Plant materials used were listed below.

Genotype	Background	References
Col-0		
cyp79B2 cyp79B3	Col-0	Zhao et al., 2002
cyp81F2 cyp81F3-2	Col-0	
cyp81F2 (SALK_123882)	Col-0	Pfalz et al., 2009
cyp81F3-2 (CS838408)	Col-0	
cyp81F4 (SALK_024438)	Col-0	Pfalz et al., 2011
cyp82C2 (GABI_261D12)	Col-0	Rajniak et al., 2015
pmr4	Col-0	Nishimura et al., 2003
sid2-2	Col-0	Wildermuth et al., 2002
pmr4 sid2-2	Col-0	
pad3-1	Col-0	Zhou et al., 1999
pen2-2 (GABI_134C04)	Col-0	Lipka et al., 2005
pen2-1 pad3-1	Col-0	Bednarek et al., 2009
cerk1-2 (GABI_096F09)	Col-0	Miya et al., 2007
fls2-1 (SALK_062054C)	Col-0	Zipfel et al., 2004

Construction of *CSEPs* transgenic lines

Arabidopsis Col-0 plants individually expressing candidate *CSEPs* with or without SP were generated by floral dip transformation with agrobacteria containing Gateway destination vectors for the indicated genes. Transformants were selected on media containing 50 μg/mL carbenicillin and 50 μg/mL hygromycin.

Fungal inoculation assay

For fungal inoculation, 7 days-old seedlings grown in half MS with 25 mM sucrose were dip-inoculated with $1.0\times10^{5\text{-}6}$ spores/mL of *Ct* or *Ci* spores for a few seconds. Plants were then transferred to Pi-deficient (50 μM KH_2PO_4) half-strength MS medium without sucrose.

Plates were placed vertically in a plant growth chamber under 16 h light/ 8 h dark at 22℃. Biomass of *Ct* or *Ci* was determined by qRT-PCR analyses for fungal *ACTIN* genes at 3 dpi. The Pi-deficient (50 μM KH_2PO_4) media contents are shown below.

Regent	Final Concentration
KH_2PO_4	50 μM
KNO_3	9.4 mM
NH_4NO_3	10.3 mM
$CaCl_2 \cdot 2H_2O$	1.5 mM
$MgSO_4 \cdot 7H_2O$	750 μM
EDTA-Na-Fe(ⅢⅠ)Salt	75 μM
$CoCl_2 \cdot 6H_2O$	55 μM
$MnCl_2 \cdot 4H_2O$	50 μM
H_3BO_3	50 μM
$ZnCl_2$	15 μM
KI	2.5 μM
$Na_2MoO_4 \cdot H_2O$	0.52 μM
KCl	575 μM
MES	1 mM
HCl	Adjust pH to 5.1
BBL Agar, Grade A (BD, #212304)	1%

Fungal growth assay *in planta* with Trp-derived secondary metabolites

Seven days-old seedlings grown in half MS with 25 mM sucrose were dip inoculated with 1.0×10^6 spores/mL of *Ct* spores for a few seconds. Plants were then transferred to the Pi-deficient (50 μM KH_2PO_4) half-strength MS media without sucrose, containing individual Trp-derived metabolites at 50 μM. Plates were placed vertically in a plant growth chamber under 16 h light/ 8 h dark at 22℃, and fungal biomass was determined at 3 dpi as described above. Metabolites used were listed as table below.

Metabolite name	Abbreviation	Provider
Indole-3-acetaldoxime	IAOx	Kyoto University, Graduate School of Engineering, Nakao Lab
Indole-3-acetonitrile	IAN	Tokyo Chemical Industry Co., Ltd.
Indole-3-acetic acid	IAA	Tokyo Chemical Industry Co., Ltd.
Indole-3-carboxylic acid	ICA	Tokyo Chemical Industry Co., Ltd.
4-hydroxyindole-3-carbonyl nitrile	4OHICN	Kyoto University, Graduate School of Engineering, Nakao Lab
Camalexin	CAM	SIGMA-ALDRICH
Indol-3-ylmethylamine	I3A	Nacalai
4-Methoxyindol-3-ylmethylamine	4MI3A	Kyoto University, Graduate School of Engineering, Nakao Lab
Indole-3-carbinol	I3C	Tokyo Chemical Industry Co., Ltd.

Fungal growth assay *in vitro* with Trp-derived secondary metabolites

Spores of *Ct* or *Ci* were dropped into Pi-deficient (50 μM KH_2PO_4) half-strength MS media without sucrose containing individual Trp-derived metabolites at 50 μM. Each droplet contained 3 μL of *Ct* or *Ci* spores at 1.0×10^6 spores/mL. Media with Dimethyl Sulfoxide (DMSO) were used as a negative control. Plates were placed horizontally in a plant growth chamber under 16 h light/ 8 h dark at 22 ℃. Colony diameter of fungi was determined at 5 days after inoculation.

Plant growth promotion (PGP) assay with *Ct*

A. thaliana seeds were placed on Pi-deficient (50 μM KH_2PO_4) half-strength MS media without sucrose. Three μL of *Ct* spores (5.0×10^3 spores/mL) were inoculated onto the media at a distance of 3.2 cm from the seeds. Plates were placed vertically in a plant growth chamber under 10 h light/ 14 h dark at 22 ℃. Shoot fresh weight (SFW) was determined at 24 dpi.

Quantitative Real-Time PCR (qRT-PCR) Analysis

Total RNA was extracted using the Sepazol-RNA I Super G (Nacalai), following by chloroform purification and isopropanol precipitation. cDNA was reversely transcribed from 500 ng total RNA using Primescript™ reverse transcriptase (Takara). qRT-PCR was performed with Power SYBR Green PCR Master Mix (Applied Biosystems, Japan) using the Thermal Cycler Dice RealTime TP870 (Takara, Japan). Expression values were normalized to that of plant *ACTIN*. *Ct or Ci ACTIN* mRNA levels were determined as an indicator for fungal biomass. The relative expression level of each gene was calculated by the $2^{-\Delta Ct}$ method. The primers used were listed as table below.

Gene	Forward primer	Reverse Primer
Plant Actin	CGGTGGTTCCATTCTTGCTTC	TGTGAACGATTCCTGGACCTG
Ct / *Ci* Actin	AGCGTGAAATCGTTCGTGAC	AAGCTCGTAGGACTTCTCCAAG
CSEP2	TGCCAAGCTCGAGGAGAA	GTCCTCCTCCGCGCTCAA
CSEP9	ACGACGAAGCTGGAGAAGAAG	ACCCGACCTCGTTTTTCTCTAC
FRK1	ATCTTCGCTTGGAGCTTCTC	TGCAGCGCAAGGACTAGAG
NHL10	TTCCTGTCCGTAACCCAAAC	CCCTCGTAGTAGGCATGAGC
CYP79B2	ACGAACAAGGCAACCCATTG	ACGGCGTTTGATGGATTGTC
CYP83B1	ACGAGACGCAAGCACTTTTG	TCTTGAGACGTGCACTGAGAC
CYP81F2	TGTCCTGGTGCGACTTTAGG	TGCACGAGTTTACGCATAGC
IGMT1	AAGTGTGGTAAGGCCTTATCC	ACCACATCTTTCAACTGTGCC

Callose Staining

Eight days-old seedlings grown in Petri dishes with liquid half MS with sucrose were treated with 10 μM flg22, 5 mg/mL chitin (NA-COS-Y), or simultaneously treated with 10 μM flg22 and 100 μM 4MI3A or 100 μM I3A or 100 μM IAOx or 100 μM I3G (Sigma) for 24 h. Seedlings were fixed, and then destained in 3:1 ethanol/acetic acid solution overnight. The fixative was changed one time. Callose staining with aniline-blue was conducted as described previously (Millet et al., 2010). Seedlings were rehydrated in 70% ethanol for 2 h, and then 50% ethanol for an additional 2 h. They were rinsed and washed overnight with water, and then treated with 10% NaOH at 37°C for 1 h to make plant tissues transparent. After washing with water three times and 150mM K_2HPO_4 once, plant tissues were incubated for at least 2 h in 150 mM K_2HPO_4 and 0.1% aniline blue (staining solution), under aluminium foil. Callose depositions were determined in a fluorescence microscope with UV lamp and DAPI filter (excitation filter 390 nm; dichroic mirror 420 nm; emission filter 460 nm). Quantification of the aniline blue-emitted fluorescence of callose deposits was conducted with ImageJ. Elicitors used were listed below.

Elicitor	Concentration	Manufacturer
flg22	10 μM	PepMic Co. Ltd. (China)
Chitin (NA-COS-Y)	5 mg/mL	Yaizu Suisankagaku Industry CO (Yaizu, Japan)

Confocal Microscopy

Seven days-old seedlings inoculated with 1.0×10^6 spores/mL of *Ct* or *Ci* spores were further growth in Pi-deficient (50 μM KH_2PO_4) half-strength MS media without sucrose for two days. Plant seedlings were treated by MA fixative (50% methanol / 10% Acetic acid / 40 % water) and then degassed once. After overnight storage at 4°C, MA fixative was removed and then washed twice with water. Periodic acid (1%) was added and degassed once, and then kept at room temperature for 20 min. Periodic acid was removed and then washed twice with

water. Schiffs reagent (100 mM $Na_2S_2O_5$, 0.15N HCl) were added and then kept at room temperature for 20 min. After removing Schiffs reagent and washing twice with water, plant cell and fungal hyphae were stained with Propidium Iodide (10 μg/mL) for 20 min. After removing PI, plant material was incubated for at least 2 h in a Glycine-NaOH buffer (Glycine 1.875 g and NaOH 0.64 g per L, pH9.5-10) and then with 0.1% aniline blue for callose staining under aluminium. Root samples were captured using the LSM710 confocal laser-scanning microscope (Zeiss). The plant cell and fungal hyphae were stained with Propidium Iodide, and excited at 561 nm by using a diode-pumped solid-state laser. Callose stained with aniline blue was excited and observed at 405 nm by using a diode laser and DAPI filter.

RESULTS

4MI3A and CAM restrict *Ct* overgrowth in *cyp79B2 cyp79B3* plants

I examined what Trp-derived metabolites have suppressive effects on *Ct* colonization by applying synthesized metabolites to the plants in fungal inoculation assays. Following inoculation with *Ct* spores, WT and *cyp79B2 cyp79B3* seedlings were grown for 3 days in low Pi (50 μM) media containing individual Trp-derived metabolites (50 μM). *Ct* biomass in roots was assessed by qRT-PCR analysis, which determined *Ct ACTIN* levels relative to plant *ACTIN* levels. In the absence of Trp-derived metabolites, *Ct* growth was dramatically increased in *cyp79B2 cyp79B3* mutants, as described previously (Hiruma et al., 2016). *Ct* overgrowth in *cyp79B2 cyp79B3* was significantly alleviated either by exogenous application of camalexin (CAM) or an IG breakdown product 4-methoxyindol-3-ylmethyl amine (4MI3A) (Figure 4). IAOx and IAN produced upstream of 4MI3A and/or CAM, respectively, in the Trp metabolic pathways, also significantly reduced *Ct* growth in *cyp79B2 cyp79B3*. These results suggest that CAM and 4MI3A, and/or their derivatives, effectively suppress *Ct* overgrowth in *A. thaliana*.

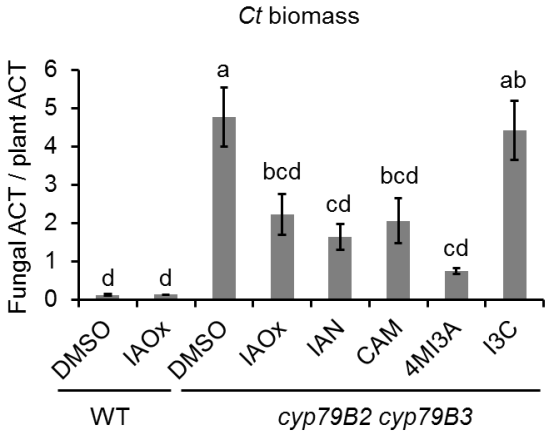

Figure 4. 4MI3A and CAM restrict *Ct* overgrowth in *cyp79B2 cyp79B3* plants.
qRT-PCR analysis for *Ct* biomass in 7 days-old WT and *cyp79B2 cyp79B3* seedlings at 3 days after application of Trp-derived metabolites at 50μM. The mean from 3 biological replicates (N = 14 per replicate) in 2 independent experiments is shown ± SE. Letters above bars indicate significantly different statistical groups, calculated with Tukey-HSD, $p < 0.05$.

4MI3A did not directly inhibit *Ct* growth in the absence of host plants.

Plant secondary metabolites often display antimicrobial activities under axenic conditions (Kliebenstein et al., 2005; Rogers et al., 1996; Sanchez-Vallet et al., 2010; Sellam et al., 2007; Wang et al., 2020). To assess whether Trp-derived metabolites have antimicrobial activity, I tested *Ct* and *Ci* growth in low Pi (50 μM) media containing Trp-derived metabolites individually. In the presence of Indole-3-acetic acid (IAA) and CAM, the medium growth of *Ct* and *Ci* was significantly suppressed, indicated by the colony diameter (Figure 5A, B and C). Indole-3-carbinol (I3C) showed a moderate inhibitory effect on *Ct* growth, but only a weak effect on *Ci* (Figure 5A, B and C), suggesting that *Ci* is more resistant to I3C compared with *Ct.* Collectively, these results suggest that IAA and CAM effectively suppress *Ct* and *Ci* growth in culture.

Interestingly, exogenous application of 4MI3A did not influence *Ct* growth under axenic conditions (Figure 5). In addition, 4MI3A did not significantly influence plant growth in the absence of fungal inoculation in low Pi (50 μM) media (Figure 6). These results suggest that 4MI3A does not directly influence *Ct* or plant growth. Importantly, 4MI3A shows an inhibitory effect of *Ct* growth only in the presence of the plant, but not on its own, suggesting that host components are required for antifungal activity of 4MI3A and/or its derivatives (Figure 4 and Figure 5). By contrast, CAM effectively inhibited *Ct* and *Ci* growth even in the absence of plants, indicating that CAM functions as an antifungal compound (Figure 5).

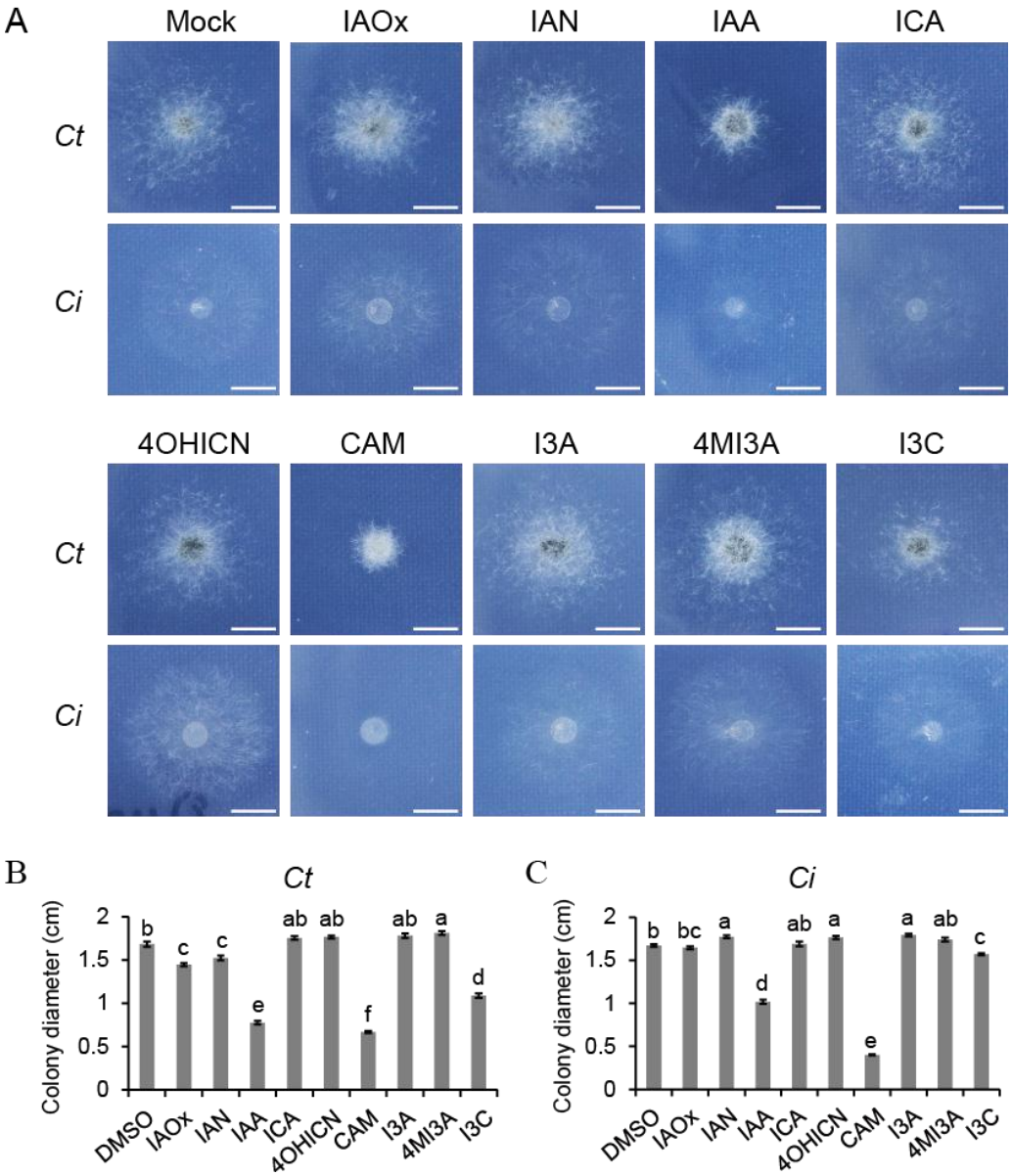

Figure 5. Effects of Trp-derived synthesized metabolites on *Ct* and *Ci* culture growth.

(A) Morphology of 5 days-old *Ct* and *Ci* colonies cultured on low Pi agar media supplemented with the indicated Trp-derived metabolites. Three μL *Ct* (1.0×10^6 spores/mL) spores were dropped onto low Pi (50 μM) media containing the indicated Trp-derived metabolites at 50 μM, and incubated for 5 days. Nine colonies were used to determine colony diameters, in two independent experiments each. Scale bars, 5 mm.

(B), (C) Diameters of *Ct* (B) and *Ci* (C) colonies with and without exogenous application of the indicated Trp-derived metabolites. Error bars indicate standard errors. Letters above bars indicate significantly different statistical groups, calculated using Tukey-HSD, $p < 0.05$.

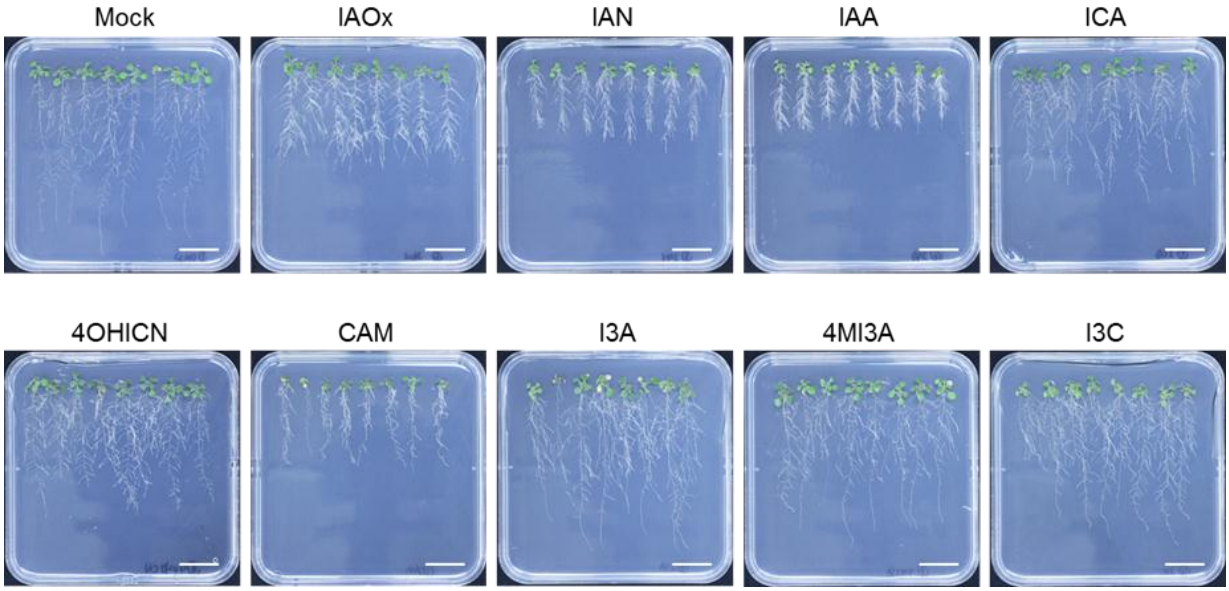

Figure 6. 4MI3A does not directly influence plant growth under low Pi conditions.
Morphology of WT plants on low Pi media with the indicated Trp-derived metabolites in the absence of fungal inoculation. Seven days-old seedlings were transferred to low Pi media (50 μM) containing 50 μM indicated Trp-derived metabolites, and further growth for 10 days. Scale bars indicate 2 cm.

CYP81F2 and *CYP81F3* in the indole glucosinolate pathway redundantly contribute to suppression of *Ct* overgrowth.

I further investigated the possible involvement of Trp-derived metabolites produced downstream of those tested above in *Ct* growth suppression. IAOx enters different metabolite pathways, which include the IG pathway that plays a role in plant defense against diverse pathogens. *CYP81F2*, *CYP81F3* and *CYP81F4* are key enzymes that mediate the hydrolysis of IG metabolite I3G (Pfalz et al., 2011). *PEN2* enzyme acts downstream of the IG pathway, and PEN2-dependent defense restricts growth of a broader spectrum of pathogens, including the nonadapted oomycete *Phytophthora infestans*, the adapted powdery mildew fungi *Golovinomyces orontii* and *G. cichoracearum*, and the necrotrophic fungus *Plectosphaerella cucumerina* (Bednarek et al., 2009; Lipka et al., 2005). *PAD3* is required for the biosynthesis of the phytoalexin camalexin (Zhou et al., 1999). *CYP82C2* encoding a cytochrome p450 and the metabolite 4-hydroxyindole-3-carbonyl nitrile (4OHICN) have been reported to enhance pathogen defense (Rajniak et al., 2015).

To gain insight into the host metabolites effectively suppressing *Ct* growth, I tested *A. thaliana* mutant lines impaired in the generation of particular subclasses of Trp-derived metabolites. Determination of fungal biomass at 3 dpi showed that *Ct* growth was significantly increased in *cyp81F2 cyp81F3* mutants, which are unable to convert I3G to 4OHI3G, compared to WT (Figure 7A), whereas there was no increase in *Ct* biomass in the

cyp81F2 or *cyp81F3* single mutants (Figure 7B). These results indicate that *CYP81F2* and *CYP81F3* redundantly contribute to suppressing *Ct* growth.

In an IG hydrolysis-defective *pen2* mutant, *Ct* biomass was not significantly affected under low Pi conditions (Figure 7B), consistent with previous studies under high Pi conditions (Hiruma et al., 2016). In the 4OHICN-defective mutant *cyp82C2*, camalexin biosynthesis mutant *pad3*, and I3G-1OHI3G conversion mutant *cyp81F4*, *Ct* growth was again not affected compared to WT (Figure 7A), suggesting that these pathways are not required for the control of *Ct* colonization under low Pi conditions.

In WT plants, 4MI3G accumulation was dramatically increased following *Ct* inoculation (Supplementary Figure 1). The results suggest that the CYP81F2/CYP81F3-mediated IG pathway is induced in response to fungal challenge, thereby restricting *Ct* colonization in roots.

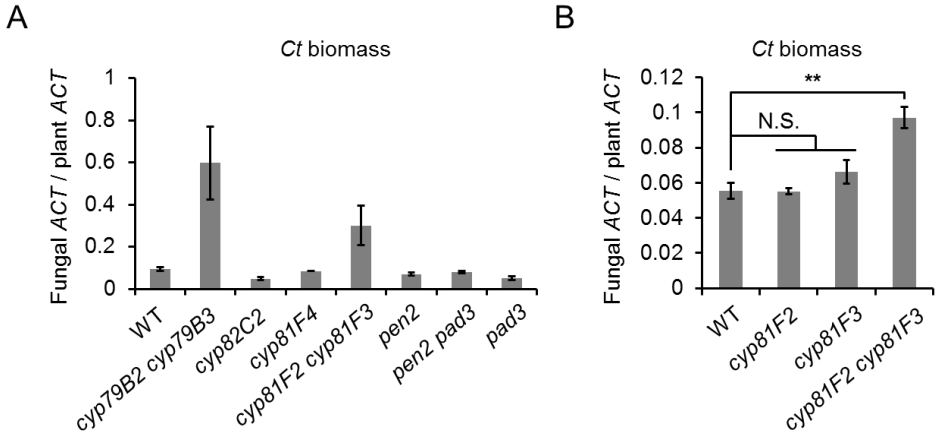

Figure 7. *CYP81F2* and *CYP81F3* redundantly restrict root colonization by *Ct*.
(A), (B) qRT-PCR analysis for *Ct* biomass in 7 days-old WT and Trp metabolite biosynthesis defective mutants at 3 dpi with *Ct*. Fungal *ACTIN* values were normalized with plant *Actin* values in 3 independent experiments of 3 biological replicates (14 seedlings per replicate) each. Error bars indicate standard errors. Asterisks indicate significant differences in the means between WT and *cyp81F2 cyp81F3* (Two-tailed t-test, $p < 0.01$). N.S. means not significant.

Ct CSEPs up-regulated in *cyp79B2 cyp79B3* plants

It is conceivable that suppression of *Ct* pathogenesis by host Trp-derived metabolites is related to the expression or function of *CSEPs*. To pursue this hypothesis, I mined the transcriptome data in the host lab of WT and *cyp79B2 cyp79B3* plants at 1 and 3 days after *Ct* inoculation. Eleven *CSEPs* were highly induced during *Ct* colonization in *cyp79B2 cyp79B3* plants compared to WT (Figure 8), suggesting that these 11 *CSEPs* are candidate effectors that render *Ct* pathogenic in *cyp79b2 cyp79b3* plants. Figure 9 shows a schematic representation of these *CSEPs*, whose sizes range from 62 to 436 amino acid length. All these *CSEPs* carry a

predicted signal peptide of 16-23 amino acids in their *N*-termini. Three *CSEPs* carry Cys residues, and *CSEP3* (CT04_01355) is Cys-rich (14 Cys residues in 133 amino acid residues), whereas the others lack Cys (Figure 9).

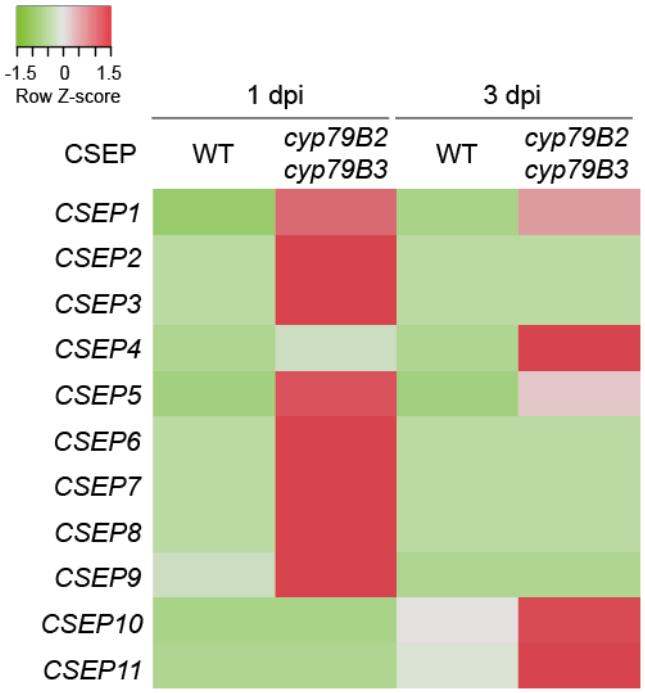

Figure 8. 11 *Ct CSEPs* were highly induced in *cyp79B2 cyp79B3* plants.
Transcriptome data analysis for WT and *cyp79B2 cyp79B3* plants at 1 and 3 days after *Ct* inoculation. Eleven *Ct CSEPs* were highly induced at either time in *cyp79B2 cyp79B3* plants compared to WT. dpi, days post inoculation.

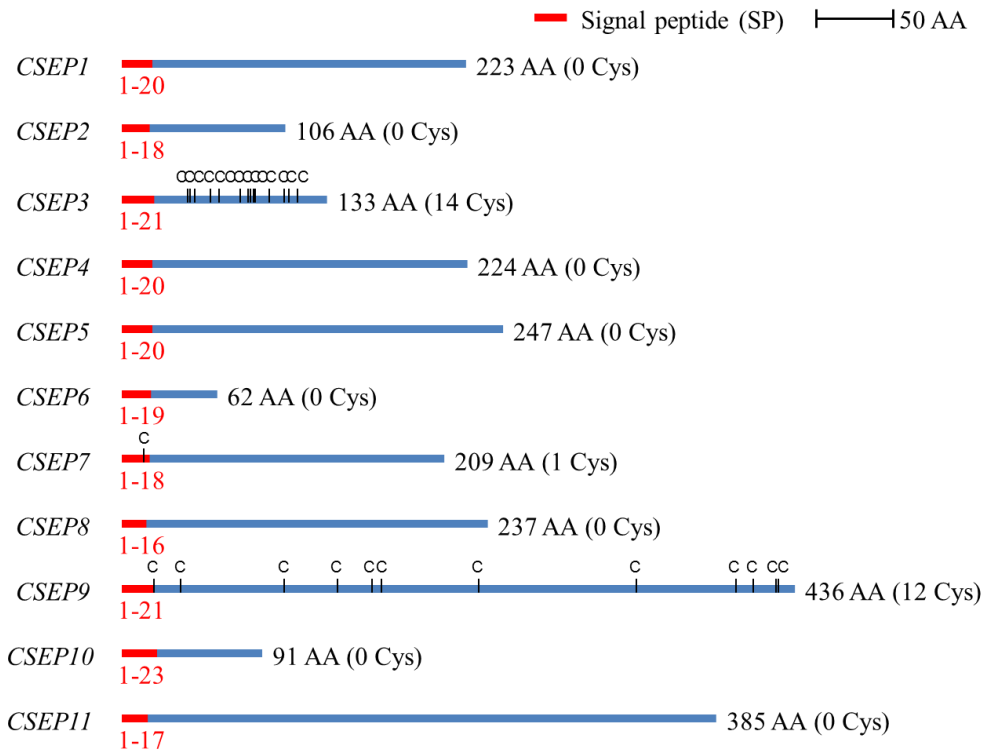

Figure 9. Schematic representation of *CSEPs* of *Ct*.
Schematic representation of *CSEPs* structures in figure 1. Coloured boxes indicate: signal peptide (red) and mature effector protein (blue). Cysteine residues (C) and the total number of amino acids (AA) are indicated.

CSEP2 and *CSEP9* contribute to *Ct* root colonization

To gain insight into functional roles for *CSEPs*, we generated transgenic Arabidopsis plants individually expressing these 11 *CSEPs* with or without signal peptide (SP) (Tsurukawa, 2020 Master thesis), as typically loss or gain of individual *CSEP* functions in fungi does not significantly affect fungal phenotypes. Two of them without SP showed increased fungal growth (Supplementary Figure 2). *Ct* biomass was significantly increased in several independent lines of the *pro35S::CSEP2ΔSP* and *pro35S::CSEP9ΔSP* (Figure 10A, B and Figure 11). I verified that *CSEP2* and *CSEP9* were highly expressed in these *pro35S::CSEP2ΔSP* and *pro35S::CSEP9ΔSP* lines, respectively (Figure 10C and D). These results suggest that the two *CSEPs* contribute to *Ct* root colonization.

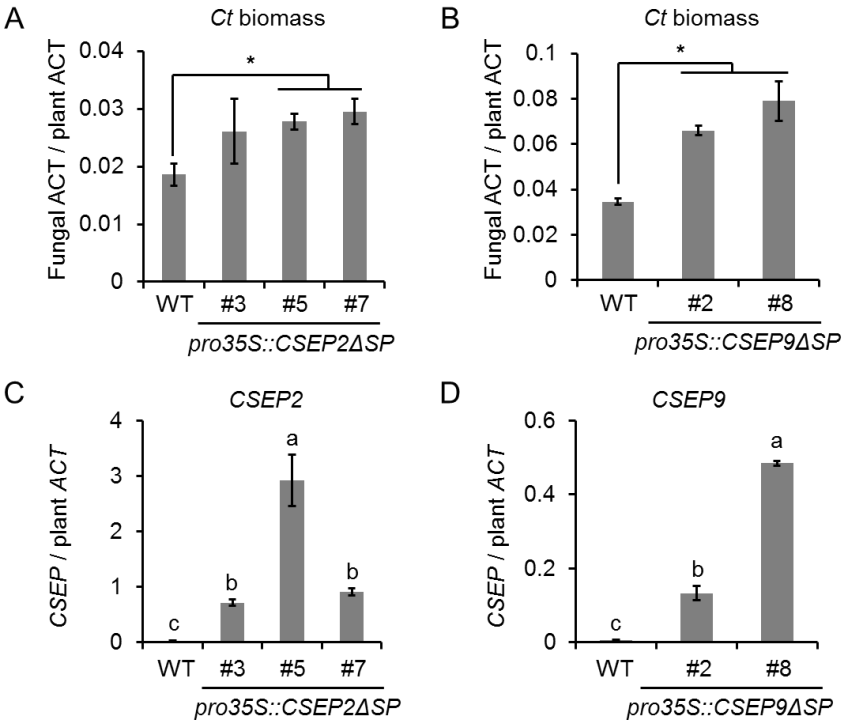

Figure 10. Two *CSEPs* contribute to *Ct* root colonization.

(A), (B) qRT-PCR analysis for *Ct* biomass in 7 days-old WT, *pro35S::CSEP2ΔSP* (A) and *pro35S::CSEP9ΔSP* (B) transgenic plants (T3 generation) at 3 dpi with *Ct*. Three or two independent *CSEP* transgenic lines were tested, respectively. Four independent experiments in (A) and 2 independent experiments in (B) were conducted with 3 biological replicates (14 seedlings per replicate) each. Error bars indicate standard errors. Asterisks indicate significant differences in the means between WT and *CSEP* transgenic plants (Two-tailed t-test, $p < 0.05$).

(C), (D) qRT-PCR analysis of *CSEP2* (C) and *CSEP9* (D) expression in 7 days-old WT, *pro35S::CSEP2ΔSP* (C) and *pro35S::CSEP9ΔSP* (D) seedlings 3 days after *Ct* inoculation. Three or two independent *CSEP* transgenic lines were tested, respectively. The data were obtained with 3 biological replicates (14 seedlings per replicate) each. Error bars indicate standard errors. Letters above bars indicate significantly different statistical groups, calculated using Tukey-HSD, $p < 0.05$.

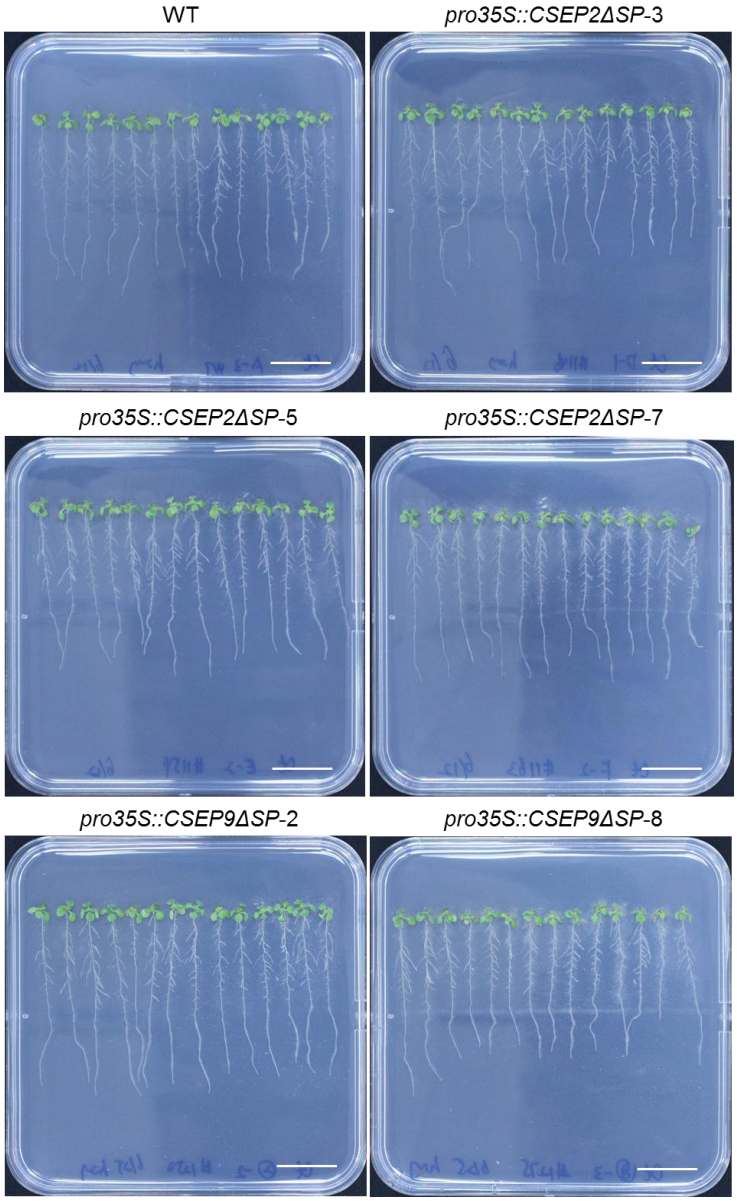

Figure 11. *pro35S::CSEP2ΔSP* and *pro35S::CSEP9ΔSP* transgenic plants following *Ct* inoculation.

Morphology of WT, *pro35S::CSEP2ΔSP* and *pro35S::CSEP9ΔSP* transgenic plants growth in low Pi media at 3 days after *Ct* inoculation. Seven days-old seedlings were dip inoculated with *Ct* spores and then further grown in low Pi media (50 μM) for 3 days. Scale bars indicate 2 cm.

CSEP2 orthologs are present in many *Colletotrichum* species

I searched homologous genes for the two *CSEPs* in different *Colletotrichum* fungi, with BLASTP searches using *Ct CSEP2* and *CSEP9* as the query sequences. In a phylogenetic tree (Gan et al., 2019), *CSEP2* homologs are widely distributed across the *Colletotrichum* genus, including *C. acutatum*, *C. spaethianum*, and *C. destructivum* (Supplementary Figure 3). In

these *Colletotrichum* species, *CSEP2* homologs show protein sequence identity ranging from 33.01% ~ 78.3%, compared to *Ct CSEP2* (Table 1). However, *CSEP9* homologs are not discernible in other *Colletotrichum* species, implying that *CSEP9* is specific to *Ct*. The results suggest that *CSEP2* is a common infection-promoting factor of *Colletotrichum* species.

Table 1. *CSEP2* orthologs in *Colletotrichum* species.

Colletotrichum species	Host plants	*CSEP2* Identity compared to *Ct*
Colletotrichum tofieldiae	*Arabidopsis thaliana*	100%
Colletotrichum incanum	Radish	78.30%
Colletotrichum shisoi	*Perilla frutescens*, *Arabidopsis thaliana*	60%
Colletotrichum higginsianum	*Arabidopsis thaliana*	60%
Colletotrichum higginsianum IMI 349063	*Arabidopsis thaliana*	60%
Colletotrichum tanaceti	Pyrethrum, Tomato, Soybean, Fabaceae	56.47%
Colletotrichum salicis	*Salix sp*.(Willow), Apple	41.59%
Colletotrichum simmondsii	Safflower	39.82%
Colletotrichum nymphaeae SA-01	Strawberries, Olives	39.82%
Colletotrichum fioriniae PJ7	Strawberry	38.94%
Colletotrichum orchidophilum	Vanilla (orchid)	39.45%
Colletotrichum camelliae	Tea plant	39.22%
Colletotrichum fructicola	Avocado, Apple, Tea plant	38.24%
Colletotrichum plurivorum	Sugarcane, Papaya, Chilli pepper, Okra	34.95%
Colletotrichum sublineola	Wild rice, Sorghum	34.88%
Colletotrichum musicola	Soybean, Taro	33.98%
Colletotrichum sojae	Soybean	33.01%

CSEP2 protein sequences are highly similar between *Ct* and *Ci*

Ct CSEP2 contains 106 amino acids without Cys, whereas *Ci CSEP2* of the same amino acid length has a Cys in the signal peptide region (Figure 12). CSEP2 protein sequences are highly similar between *Ct* and *Ci*, with 78.3% identity at the amino acid level (Figure 12).

Signal peptide

```
Ct CSEP2   1  MRFNNLLAVFSFVTGALAAKYILVLNASTDVDDFSAKLEEKDIDVLAKFPFFK  53
Ci CSEP2   1  MRFTNLFTVFSCVAGALAAKYILVLDPSTDIDGFIAKLEENEIDVLTKFPLFK  53

Ct CSEP2  54  ILVVETDSHDVAALEAYDEVLSAEEDQDSSIGPLPTSSEPLPVDTPFPLPGWS  106
Ci CSEP2  54  ILVVETNSHDIAALESYDEVLSAEEDQISSIDPPPSSPEPLPVETPFPLPGWS  106
```

Figure 12. CSEP2 protein sequences are highly similar between *Ct* and *Ci*.
Protein sequences of CSEP2 in *Ct* and *Ci*. The predicted signal peptide of both *Ct* and *Ci* contain 18 amino acid sequences. Black letters indicate conserved amino acid sequences. Red letters denote variations between *Ct* and *Ci*. *Ct* CSEP2 and *Ci* CSEP2 display 78.3% identity at the protein sequence level.

Expression of *Ci CSEP2* ortholog in *Ci* is correlated with increased fungal biomass

To test possible correlation of *CSEP2* expression with fungal pathogenesis in *Ci*, I compared *CSEP2* expression in *Ct* and *Ci* when inoculated onto WT plants. I confirmed that *Ci* biomass was greater than that of *Ct* in all the tested time points (Figure 13A). *CSEP2* expression was also dramatically increased in *Ci* compared to *Ct* at the tested time points (Figure 13B). These results suggest that *CSEP2* expression in *Ci* is correlated with fungal growth in plants.

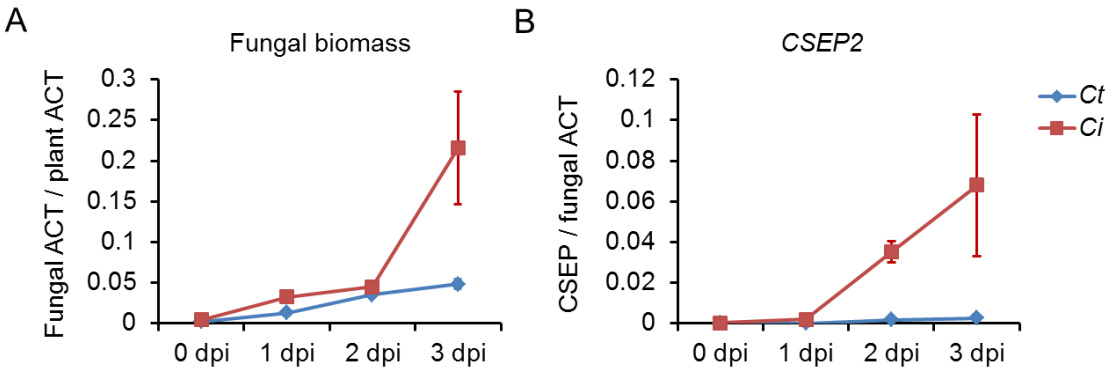

Figure 13. Expression of *CSEP2* ortholog in pathogenic *Ci* is associated with increased fungal biomass in WT plants.
(A), (B) qRT-PCR analysis of fungal biomass (A) and *CSEP2* expression (B) in 7 days-old WT seedlings at the indicated times after *Ct* or *Ci* inoculation. The data were obtained with 3 biological replicates (14 seedlings per replicate) each. dpi, day after inoculation. Error bars indicate standard errors.

4MI3A and CAM suppress *CSEP2* expression in *cyp79B2 cyp79B3* plants

Exogenous application of Trp-derived metabolites 4MI3A and CAM, restricting *Ct* overgrowth, also effectively suppressed *Ct CSEP2* expression in *cyp79B2 cyp79B3* plants (Figure 4 and Figure 14), pointing to correlation between *CSEP2* expression and fungal overgrowth and pathogenesis.

In addition, introduction of *CSEP2* did not influence plant growth in the absence of *Ct* (Figure 15).

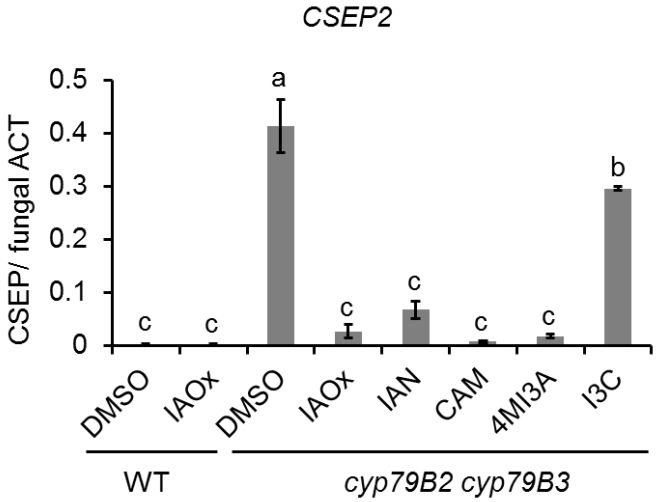

Figure 14. 4MI3A and CAM application suppresses *CSEP2* expression in *cyp79B2 cyp79B3* plants.

qRT-PCR analysis for *Ct CSEP2* expression in 7 days-old WT and *cyp79B2 cyp79B3* seedlings, applied with the indicated Trp-derived metabolites (50μM) at 3 days after *Ct* inoculation. Relative expression values were calculated with fungal *ACTIN* values as the standard, with 3 biological replicates (14 seedlings per replicate). Error bars indicate standard errors. Letters above bars indicate significantly different statistical groups, calculated with Tukey-HSD, $p < 0.05$.

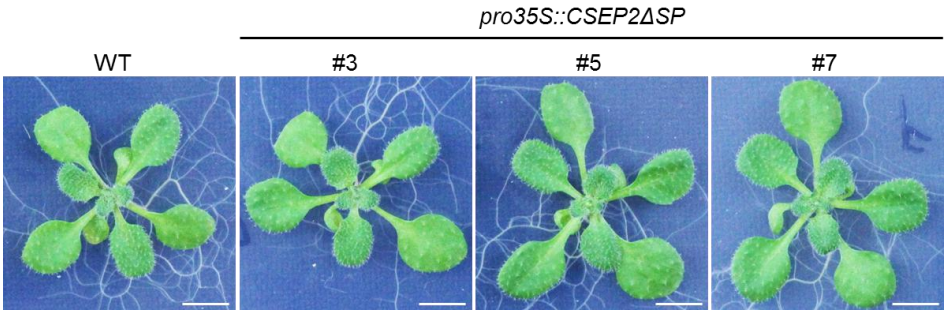

Figure 15. Introduction of *CSEP2* does not influence plant growth in the absence of *Ct*.
Morphology of 15-day-old WT and *pro35S::CSEP2ΔSP* transgenic plants grown in half MS media with sucrose in the absence of *Ct*. Scale bars indicate 5 mm.

Overexpression of *CSEP2* in *Arabidopsis* does not influence MAMP induction of defense-related genes

Putative *CSEP2* orthologues are present in many *Colletotrichum* species and *Ct CSEP2* contributes to *Ct* root colonization. This prompted me to test whether *CSEP2* targets plant immune responses that restrict potential pathogenesis or growth of *Ct*. First, I tested the expression level of *FRK1* and *NHL10*, two MAMP-inducible defense-related genes, at 3 h after treatment with chitin (200 μg/mL, Sigma) or flg22 (1 μM). *FRK1* and *NHL10* induction was not significantly altered in *pro35S::CSEP2ΔSP* plants compared to WT plants in response to either MAMP (Figure 16A and B), implying a minor effect of *CSEP2* on MAMP induction of defense-related genes.

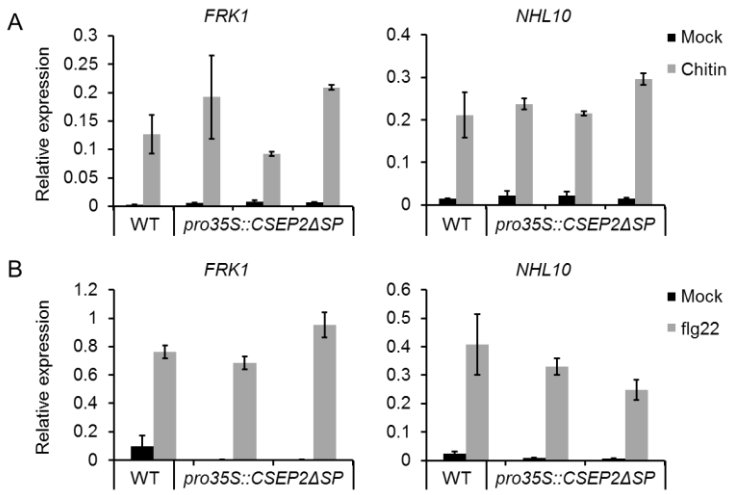

Figure 16. Overexpression of *CSEP2* in *Arabidopsis* does not influence MAMP-induced expression of defense-related genes.

(A), (B) qRT-PCR analysis for *FRK1* and *NHL10* in 7 days-old WT and *pro35S::CSEP2ΔSP* transgenic plants treated with 200 μg/mL chitin (A) and 1 μM flg22 (B). Seven days-old seedlings from half MS agar medium were transferred to half MS liquid medium for 1 day, followed with MAMPs treatments for 3 h. *FRK1* and *NHL10* were MAMP-triggered PTI-associated marker genes. The data were obtained in 3 biological replicates (10 seedlings per replicate) each. Error bars indicate standard errors.

CSEP2 suppressed MAMP-induced callose deposition in *Arabidopsis* roots

Next, I tested possible *CSEP2* effects on another representative PTI output, callose deposition. Callose deposition is induced in leaves and roots in response to different MAMPs, and is thought to strengthen cell wall-based defense (Luna et al., 2011). In *A. thaliana* roots, flg22-induced callose deposition occurs in the epidermal layer in the elongation zone, whereas chitin-elicited callose deposition occurs throughout the entire mature zone (Millet et al., 2010).

Here, I compared MAMP-triggered callose deposition between WT and *pro35S::CSEP2ΔSP* transgenic plants. *pro35S::CSEP2ΔSP* showed decreased flg22-induced callose deposition relative to WT plants at the root differentiation zone (Figure 17A and C). Callose deposition was completely abolished in *fls2*, an flg22 receptor mutant, confirming the specificity of the observed flg22 responses (Figure 17A and C). Chitin-elicited callose deposition was also decreased in *pro35S::CSEP2ΔSP* roots compared to WT, and was abolished in the *cerk1* mutant that is insensitive to chitin (Figure 17B and D). These results indicated that overexpression of *CSEP2* in *A. thaliana* attenuated MAMP-induced callose deposition in roots. By contrast, an introduction of *Ct*-specific *CSEP9* did not influence flg22-induced callose deposition in roots (Figure 18A and B). These results suggested that *CSEP2*, which is conserved in many *Colletotrichum* species, but not *Ct* specific *CSEP9*, specifically attenuates callose deposition in roots during PTI.

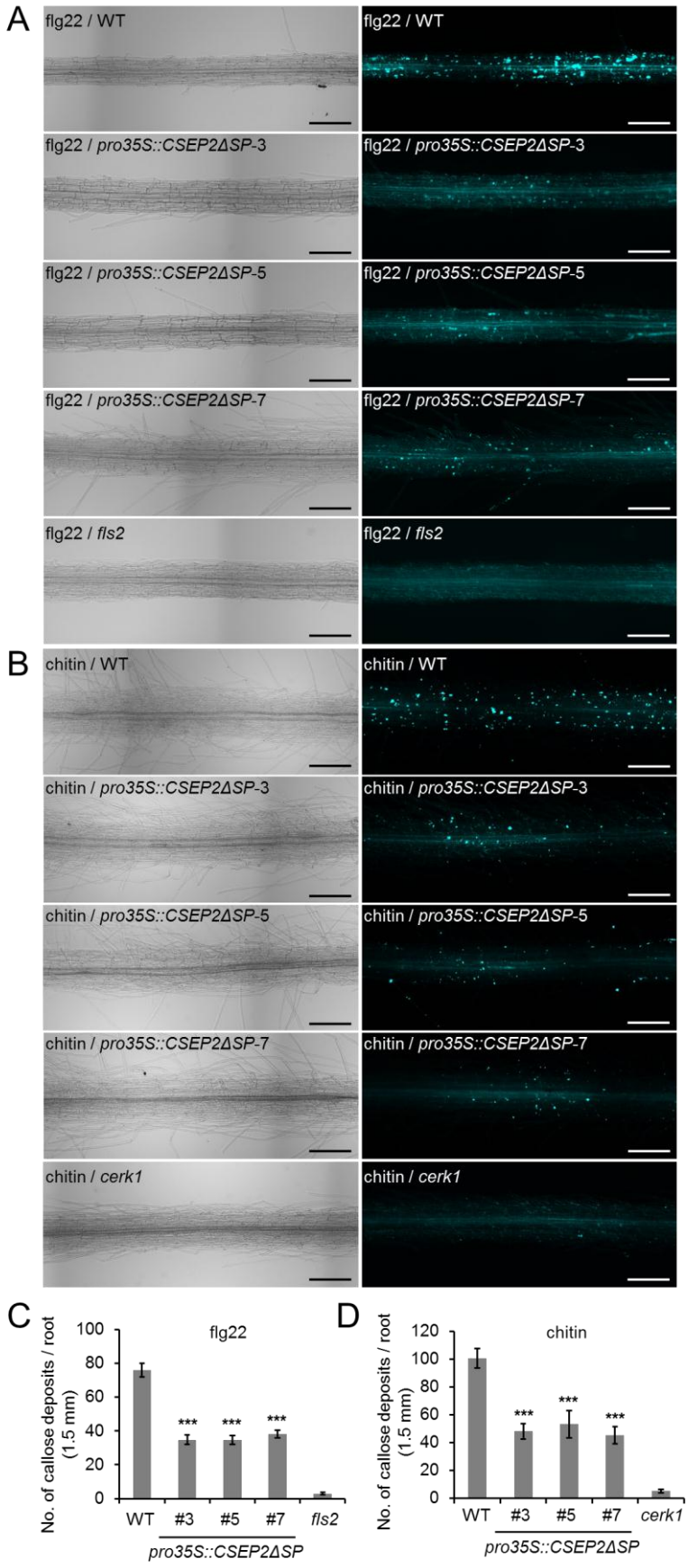

Figure 17. Introduction of *CSEP2* diminished MAMP-induced callose deposition in *Arabidopsis* roots.

(A), (B) MAMP-induced callose deposition in 8 days-old WT, *pro35S::CSEP2ΔSP*, *fls2* and *cerk1* seedlings. Eight days-old seedlings were treated with 10 μM flg22 (A) and 5 mg/mL chitin (B) for 24h. Three independent *CSEP2* transgenic lines were used. *fls2*, flg22 receptor mutant. *cerk1*, chitin receptor mutant. Four independent experiments in (A) and two independent experiments in (B) were repeated with the same conclusions, and representative results are shown. Scale bar, 200 μm. The same conclusions were obtained with 1 μM or 5 μM flg22, or 10 mg/mL chitin (not shown).

(C), (D) Number of callose deposits in WT, *pro35S::CSEP2ΔSP*, *fls2* and *cerk1* roots response to flg22 (C) and chitin (D) presented in (A) and (B), respectively. Number of callose deposits was quantified as the number of fluorescent callose in a 1.5 mm differentiation zone (C) and 1.5 mm mature zone (D) of roots, using Image J. Results of four independent experiments in (C, N = 43-50) and two independent experiments in (D, N = 20-23) were combined. Error bars indicate standard errors. Asterisks indicate significant differences in the means between WT and *pro35S::CSEP2ΔSP* transgenic plants (Two-tailed t-test, $p < 0.001$).

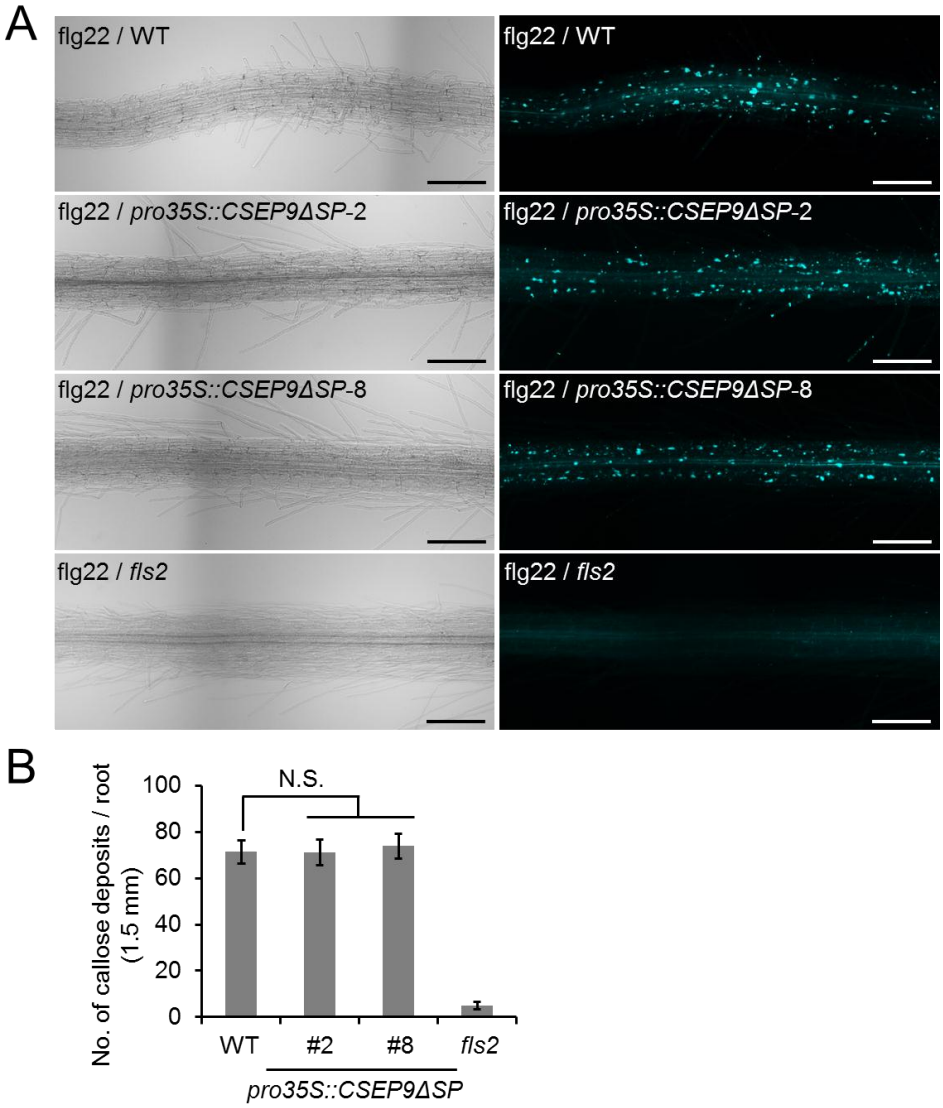

Figure 18. Introduction of *CSEP9* does not influence flg22-induced callose deposition in *Arabidopsis* roots.

(A) flg22-induced callose deposition in 8 days-old WT, *pro35S::CSEP9ΔSP*, and *fls2* seedlings treated with flg22 before aniline blue staining. 8 days-old seedlings from half MS liquid medium were treated with 10 μM flg22 for 24h. Two independent *CSEP9* transgenic lines were detected. *fls2*, flg22 receptor mutant. Two independent experiments were conducted. Scale bar, 200 μm.

(B) Number of callose deposits in WT, *pro35S::CSEP9ΔSP*, and *fls2* roots presented in (A). Number of callose deposits was determined by counting the number of fluorescent callose per root. 1.5 mm differentiation zone of per root was calculated using Image J. Results of two independent experiments (N = 21-26) were combined. Error bars indicate standard errors. N.S. indicates no significant differences in the means between WT and *pro35S::CSEP9ΔSP* transgenic plants (Two-tailed t-test).

IG biosynthesis and hydrolysis are required for flg22-induced callose in *Arabidopsis* roots

I confirmed that flg22-induced callose deposition in root differentiation zones was reduced in the IG biosynthesis mutants *cyp79B2 cyp79B3* and *cyp81F2 cyp81F3*, as well as in *pen2* (Figure 19A and B), which is consistent with previous works (Clay et al., 2009; Millet et al., 2010).

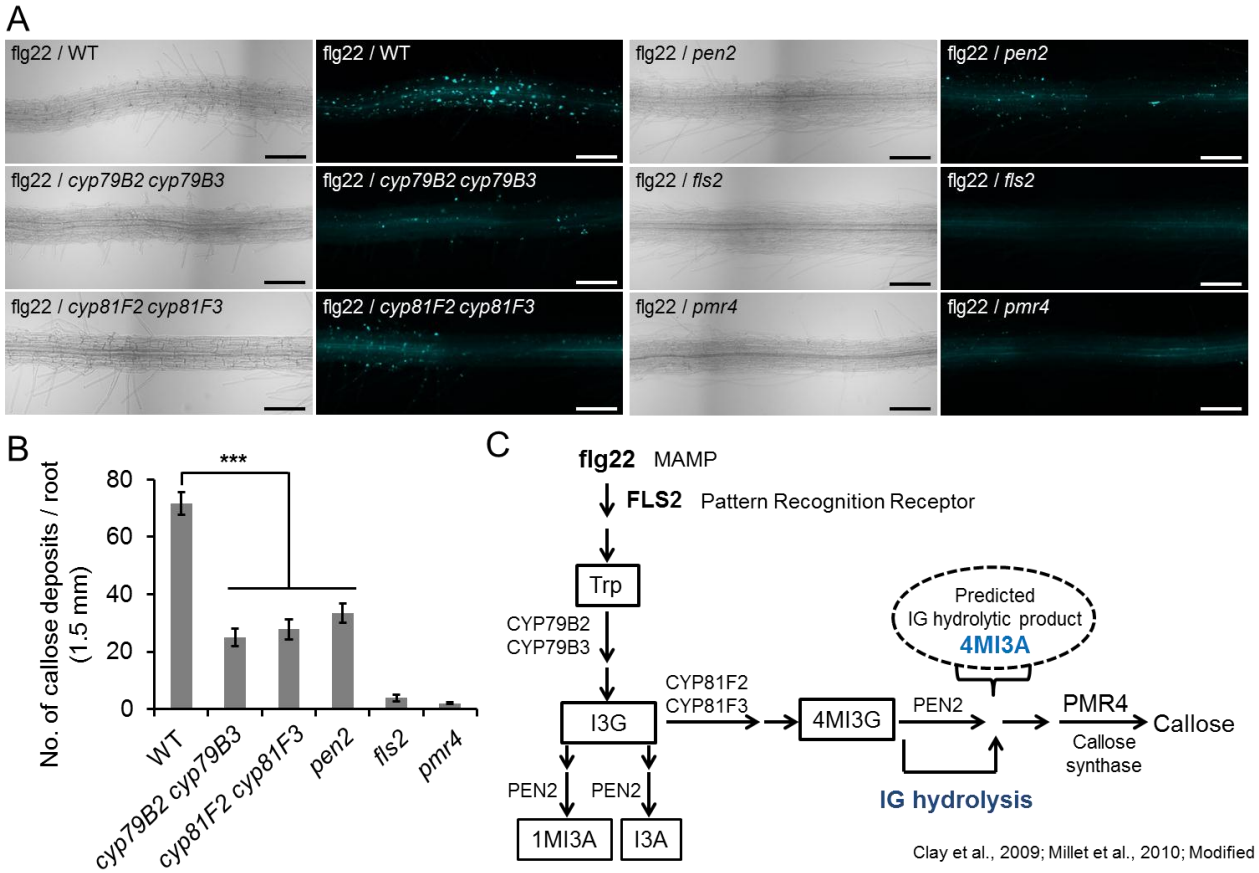

Figure 19. IG biosynthesis and hydrolysis are required for flg22-induced callose formation in *Arabidopsis* roots.

(A) flg22-induced callose deposition in 8 days-old WT, *cyp79B2 cyp79B3*, *cyp81F2 cyp81F3*, *pen2*, *fls2* and *pmr4* seedlings. Representative images of three independent experiments are shown. Scale bar, 200 μm.

(B) Number of callose deposits in (A). 1.5 mm differentiation zone of the roots, determined using Image J. Results of three independent experiments (N = 27-34) were combined. Error bars indicate standard errors. Asterisks indicate significant differences in the means between WT and IG-related mutant plants (Two-tailed t-test, $p < 0.001$).

(C) A model for MAMP-induced callose deposition in Arabidopsis (Clay et al., 2009; Millet et al., 2010, modified).

4MI3A restores flg22-induced callose formation in *pro35S::CSEP2ΔSP* and IG biosynthesis mutants

flg22 perception is expected to induce CYP81F2-dependent 4MI3G production, followed by 4MI3G hydrolysis to produce callose-eliciting compounds(s) (Figure 19C) (Clay et al., 2009; Millet et al., 2010). 4MI3G application restores flg22-induced callose formation in leaves of *cyp79B2 cyp79B3* and *cyp81F2*, albeit not in *pen2* (Clay et al., 2009). However, a presumed IG hydrolytic product 4-methoxy-indole-3-acetonitrile (4MI3A), purified from Chinese cabbage, and IG hydrolytic products, 4-methoxy-indole-3-carboxylate and methyl-4-methoxy-indole-3-carboxylate, failed to rescue these mutants (Clay et al., 2009).

4MI3A is predicted to be derived from 4MI3G, through hydrolysis via PEN2 myrosinase (Bednarek et al., 2009; Clay et al., 2009). I tested whether exogenous 4MI3A application restores callose deposition in roots of IG biosynthetic and hydrolytic mutants. Simultaneous application of 100 μM 4MI3A with 10 μM flg22, recovered callose deposition in *cyp79B2 cyp79B3* and *cyp81F2 cyp81F3*, but not in *pen2*, *fls2*, or *pmr4* (Figure 20A and C). 4MI3A *per se* did not induce callose formation in the absence of flg22 (Figure 21). The results indicate that 4MI3A is required for flg22-induced callose deposition in roots. The failure for 4MI3A to rescue *pen2* implies the requirement for another critical metabolite(s) produced by PEN2 myrosinase in callose formation (See Figure 1).

Remarkably, 4MI3A application restored flg22-induced callose formation in *pro35S::CSEP2ΔSP* plants (Figure 20A and B). However, I3A, a metabolite produced in a parallel IG branch with the 4MI3A branch, did not recover flg22-induced callose formation in *pro35S::CSEP2ΔSP* plants (Figure 22A). This implies that *CSEP2* negatively influences some step upstream of 4MI3A production in this IG biosynthesis branch, and that this *CSEP2* function but not *CSEP2* expression is attenuated by 4MI3A application. I am currently testing possible 4MI3A effects on *CSEP2* expression in *pro35S::CSEP2ΔSP* plants.

By contrast, IAOx application did not restore flg22-induced callose formation in *pro35S::CSEP2ΔSP* transgenic plants (Figure 23), implying the existence of a *CSEP2* target step downstream of IAOx production. To further narrow down the target step of *CSEP2* in the IG pathway, I tested the possible effects of I3G, an intermediate located downstream of IAOx and upstream of 4MI3A, on flg22-induced callose deposition in *pro35S::CSEP2ΔSP* and IG-related mutants. I3G restores flg22-induced callose deposition in *cyp79B2 cyp79B3*, but not in *pro35S::CSEP2ΔSP*, *cyp81F2 cyp81F3* and *pen2* (Figure 24), suggesting that *CSEP2* interferes some step downstream of I3G production. Overall, It seems likely that *CESP2* interferes with some step downstream of I3G but upstream of 4MI3A production in the IG pathway, for suppressing MAMP-induced callose deposition.

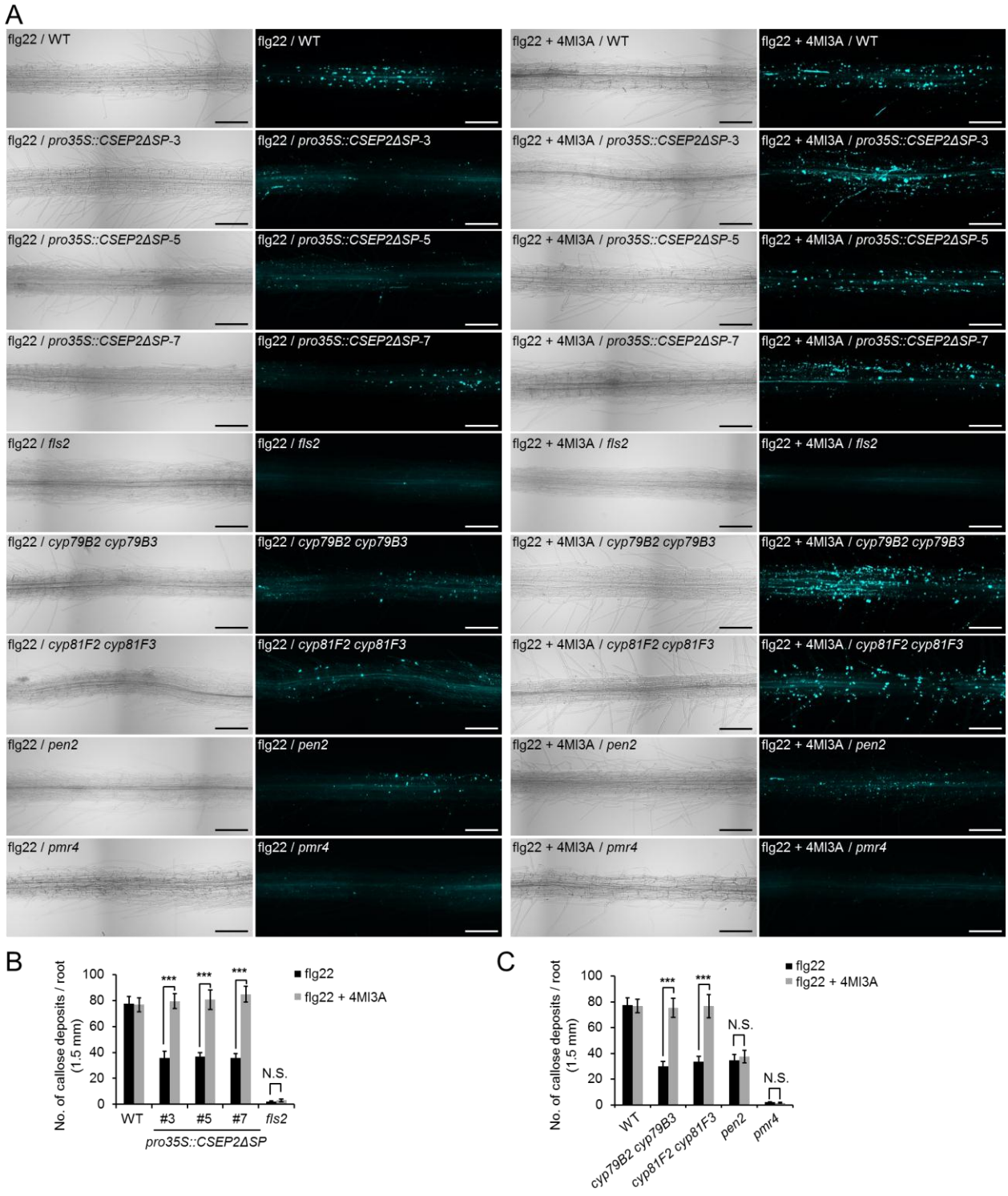

Figure 20. 4MI3A restores flg22-induced callose formation in *pro35S::CSEP2ΔSP* and IG biosynthetic mutants.

(A) Callose deposition in 8 days-old WT, *pro35S::CSEP2ΔSP*, *fls2*, *cyp79B2 cyp79B3*, *cyp81F2 cyp81F3*, *pen2*, and *pmr4* seedlings exposed to 10 μM flg22 with or without 100 μM 4MI3A before aniline blue staining. Two independent experiments were conducted. Scale bar, 200 μm.

(B), (C) Number of callose deposits in WT, *pro35S::CSEP2ΔSP*, *cyp79B2 cyp79B3*, *cyp81F2*

cyp81F3, *pen2*, *fls2* and *pmr4* roots presented in (A). Number of callose deposits was determined as the number of fluorescent callose in each root in 1.5 mm differentiation zone, using Image J. Results of two independent experiments (N = 17-26) were combined. Error bars indicate standard errors. Asterisks indicate significant differences in the means between flg22 and flg22 + 4MI3A treated plants (Two-tailed t-test, $p < 0.001$). N.S. means not significant.

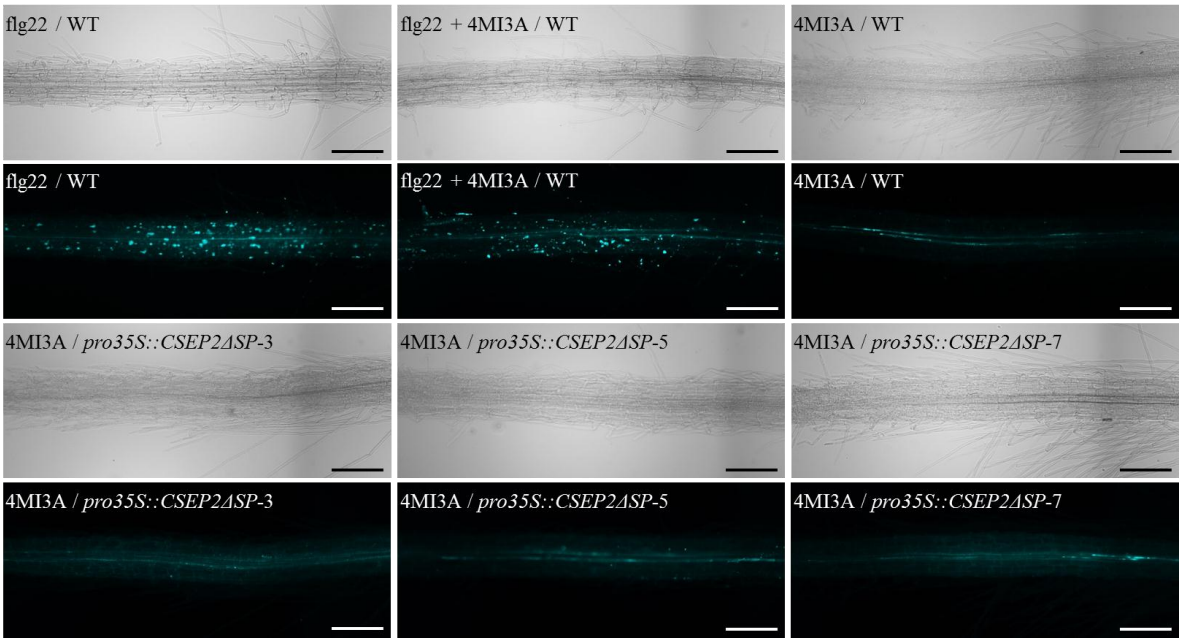

Figure 21. 4MI3A does not induce callose in non-elicited roots.

(A) flg22-induced callose deposition in 8 days-old WT and *pro35S::CSEP2ΔSP* transgenic plant roots treated with flg22, 4MI3A, or both for 24 h before aniline blue staining. N = 8-12. Scale bar, 200 μm.

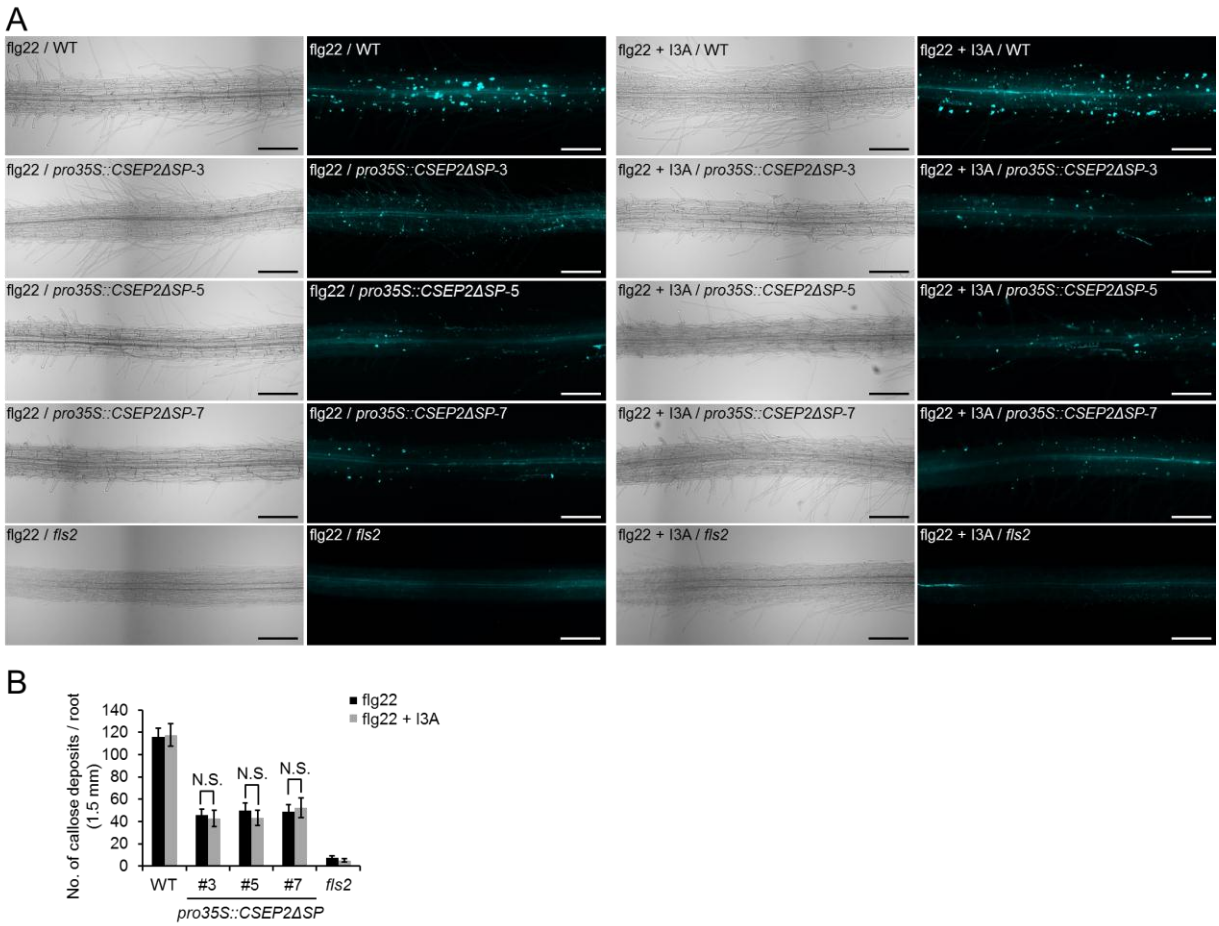

Figure 22. I3A does not rescue flg22-induced callose formation in *pro35S::CSEP2ΔSP* transgenic plants.

(A) flg22-induced callose deposition in 8 days-old WT, *pro35S::CSEP2ΔSP* and *fls2* seedlings exposed to 10 μM flg22 with or without 100 μM I3A for 24h, before aniline blue staining. *fls2*, flg22 receptor mutant. Two independent experiments were conducted. Scale bar, 200 μm.

(B) Number of callose deposits in WT, *pro35S::CSEP2ΔSP* and *fls2* roots presented in (A). Number of callose deposits per root was determined in a 1.5 mm differentiation zone, with Image J. Results of two independent experiments (N = 18-28) were combined. Error bars indicate standard errors. N.S. indicates no significant differences in the means between I3A-treated and untreated plants (Two-tailed t-test).

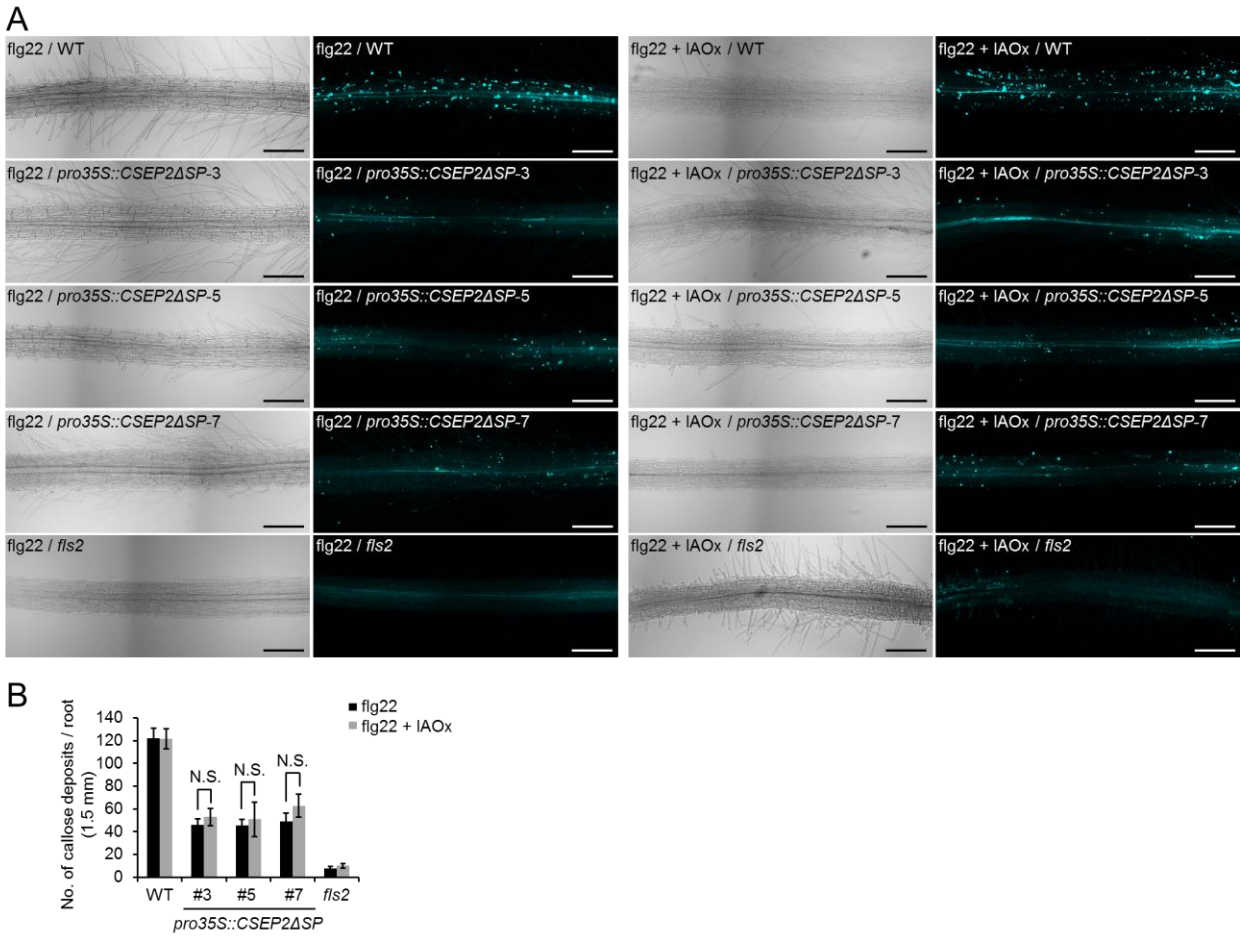

Figure 23. IAOx does not rescue flg22-induced callose formation in *pro35S::CSEP2ΔSP* transgenic plants.

(A) flg22-induced callose deposition in 8 days-old WT, *pro35S::CSEP2ΔSP* and *fls2* seedlings exposed to 10 µM flg22 with or without 100 µM IAOx for 24h, before aniline blue staining. Scale bar, 200 µm.

(B) Number of callose deposits in WT, *pro35S::CSEP2ΔSP* and *fls2* roots presented in (A). Number of callose deposits was determined by counting the number of fluorescent callose per roots under microscopy, in 1.5 mm differentiation zone of the root, using Image J. N = 12-21. Error bars indicate standard errors. N.S. indicates no significant differences between IAOx-treated and untreated plants (Two-tailed t-test).

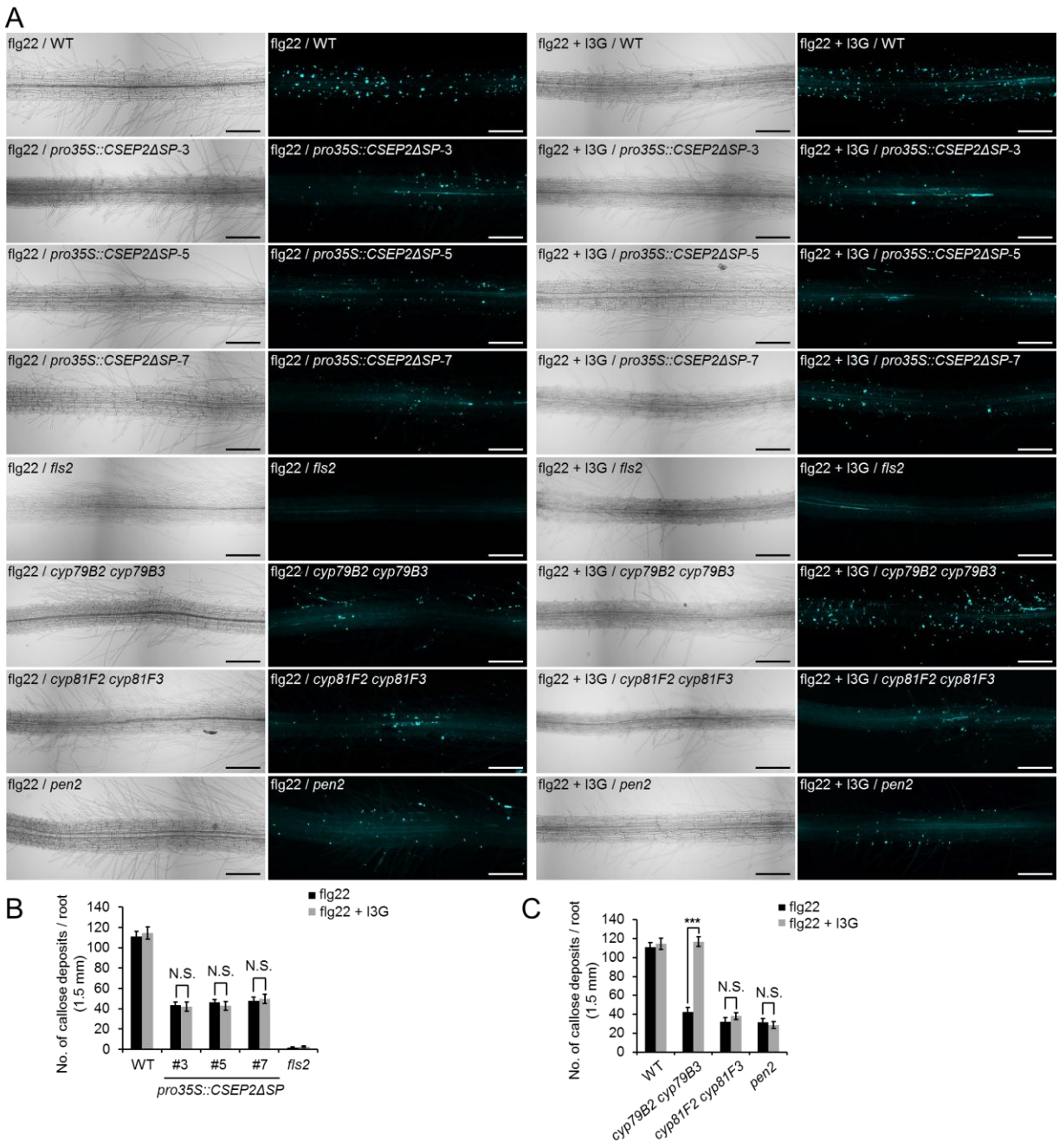

Figure 24. I3G restores flg22-induced callose formation in *cyp79B2 cyp79B3*, but not in *pro35S::CSEP2ΔSP* and *cyp81F2 cyp81F3*.

(A) Callose deposition in 8 days-old WT, *pro35S::CSEP2ΔSP*, *fls2*, *cyp79B2 cyp79B3*, *cyp81F2 cyp81F3*, and *pen2* seedlings exposed to 10 µM flg22 with or without 100 µM I3G before aniline blue staining. Scale bar, 200 µm.

(B), (C) Number of callose deposits in WT, *pro35S::CSEP2ΔSP*, *fls2*, *cyp79B2 cyp79B3*, *cyp81F2 cyp81F3* and *pen2* roots presented in (A). Number of callose deposits per root was determined in a 1.5 mm differentiation zone, using Image J. N = 20-26. Error bars indicate standard errors. Asterisks indicate significant differences in the means between flg22 and flg22 + I3G treated plants (Two-tailed t-test, $p < 0.001$). N.S. means not significant.

CSEP2 does not influence IG-related genes expression in response to flg22

I next assessed whether *CSEP2* suppresses expression of IG-related genes, by examining *CYP79B2*, *CYP83B1*, *CYP81F2* and *IGMT1* expression in WT and *pro35S::CSEP2ΔSP* plants in response to flg22. None of these genes exhibited significant differences in flg22 induction between the two genotypes at the tested time points (Figure 25). These results suggest that *CSEP2* does not prominently influence flg22 induction of IG-related genes.

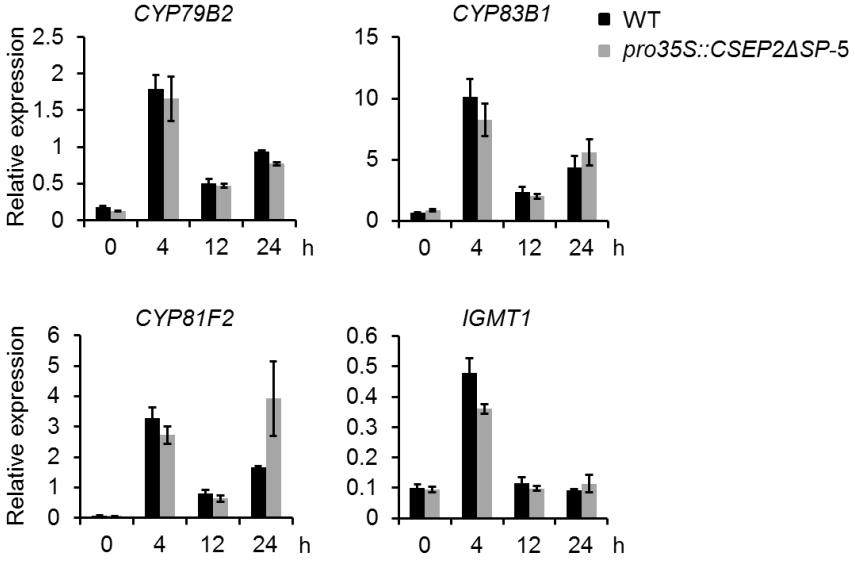

Figure 25. Expression of IG-related genes is not significantly affected by transgenic *CSEP2* introduction in *Arabidopsis* seedlings.
qRT-PCR analysis for IG-related gene expression in 8 days-old WT and *pro35S::CSEP2ΔSP* seedlings when exposed to 1 μM flg22 for the indicated times. Relative expression values were determined with *ACTIN* as the standard, and means from 3 biological replicates (n = 12) shown. Error bars indicate standard errors.

PMR4-dependent callose deposition is induced at *Ct* penetration sites

Callose papillae typically appear around the penetration sites in leaves when challenged with powdery mildew fungi, but are dramatically reduced or absent in *pmr4* (Nishimura et al., 2003). By contrast, elevated callose deposition in PMR4-overexpression plants is associated with penetration defects of powdery mildew fungi (Ellinger et al., 2013). This is consistent with the notion that *PMR4*-dependent callose-rich papillae contributes to fungal penetration resistance. However, loss of *PMR4* function also results in strong powdery mildew resistance, presumably as a consequence of backup defense activation (Aist, 1976; Ellinger et al., 2013; Nishimura et al., 2003; Voigt, 2014).

I examined whether *Ct* and *Ci* infection induces callose deposition at the penetration sites in roots. In WT plants, *Ct* and *Ci* penetration both results in callose deposition around their penetration sites (Figure 26A and C). *Ct*-induced callose deposition was absent in *pmr4*

(Figure 26B), validating that this callose deposition in roots is also *PMR4* dependent.

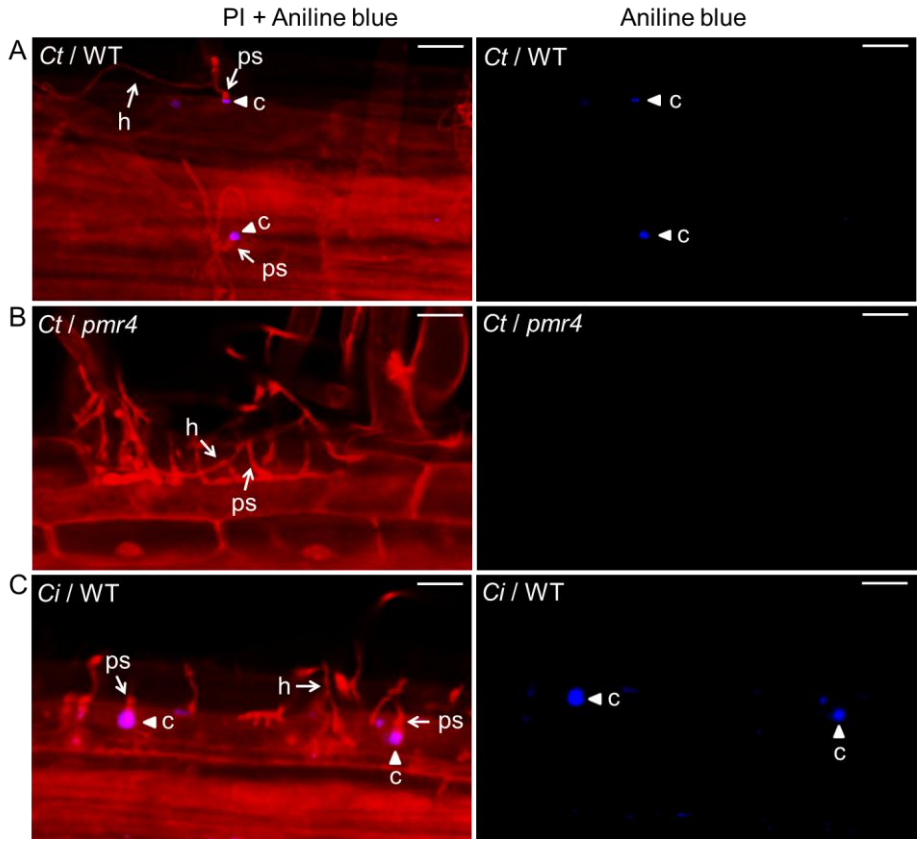

Figure 26. *Ct*/*Ci*-induced callose deposition at fungal papillae sites in *Arabidopsis* roots. (A), (B) Callose deposition at fungal papillae sites at 2 days after *Ct* (A) and *Ci* (B) inoculation in Col-0 roots under low Pi conditions (50 μM). (C) Callose deposition at papillae sites at 2 days after *Ct* inoculation in *pmr4* under low Pi conditions (50 μM). (A-C) Callose (c, stained with aniline blue) at *Ct* penetration sites is not seen in *pmr4*. Plant cells and fungal hyphae (h) were stained with propidium iodide (red fluorescence). Penetration sites (ps) are indicated by arrows. Callose deposits are indicated by arrowhead. Scale bar, 20 μm.

Ct, but not *Ci*, increased fungal growth in *pmr4* callose synthase mutants

To assess possible roles for *PMR4*-mediated callose deposition in interactions with endophytic and pathogenic fungi, I examined *Ct* and *Ci* growth in WT and *pmr4* plants. In *pmr4*, *Ct* biomass was increased compared with WT under low Pi conditions, whereas it was not affected in *sid2* lacking a major branch of defense-inducible SA biosynthesis (Figure 27A). By contrast, *Ci* biomass was not affected in *pmr4* or *sid2* (Figure 27B). It should also be noted that *pmr4* mutants did not exhibit increased resistance to *Ct* or *Ci*, in contrast to the previously described, SA-dependent resistance to leaf-infecting fungal pathogens (Nishimura et al., 2003). Consistently, increased *Ct* growth in *pmr4* was not affected by simultaneous disruption of *SID2*, indicated by the increased fungal biomass in *pmr4 sid2* compared to *sid2* (Figure 27A). Thus, SA is unlikely to play a major role in the control of endophytic or pathogenic fungal growth in roots. These results suggest that callose deposition specifically

limits *Ct* growth in roots in a manner independent of SA.

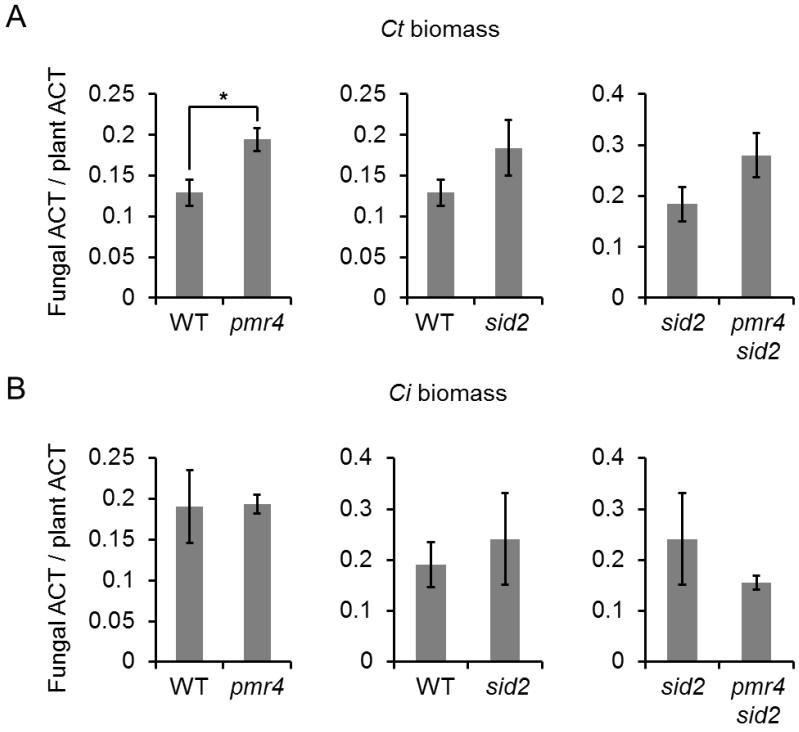

Figure 27. Callose synthase mutant *pmr4* showed increased *Ct* biomass.
(A), (B) qRT-PCR analysis for *Ct* (A) and *Ci* (B) biomass in 7 days-old WT, *pmr4*, *sid2* and *pmr4 sid2* seedlings at 3 days after inoculation under low Pi conditions (50 μM). Relative expression levels of fungal *ACTIN* to plant *ACTIN* were determined in 3 independent experiments with 3 biological replicates (N = 14) each. Error bars indicate standard errors. Asterisks indicate significantly different statistical groups, calculated with two-tailed t-test, $p < 0.05$.

CSEP2 overexpression alone is not sufficient to impair plant growth promotion by *Ct*

Having shown that *CSEP2* suppresses MAMP-induced callose deposition and promotes *Ct* infection in roots (Figures 10 and 17), I tested whether *CSEP2* influences *Ct*-mediated plant growth promotion under low Pi conditions. At 24 dpi, *Ct*-mediated plant growth promotion was retained in *pro35S::CSEP2ΔSP* transgenic plants as well as in WT plants (Figure 28 A). Shoot fresh weight (SFW) with or without *Ct* was similar between *pro35S::CSEP2ΔSP* transgenic plants and WT (Figure 28 B). The results indicate that *CSEP2* alone is not sufficient to impair plant growth promotion by *Ct*.

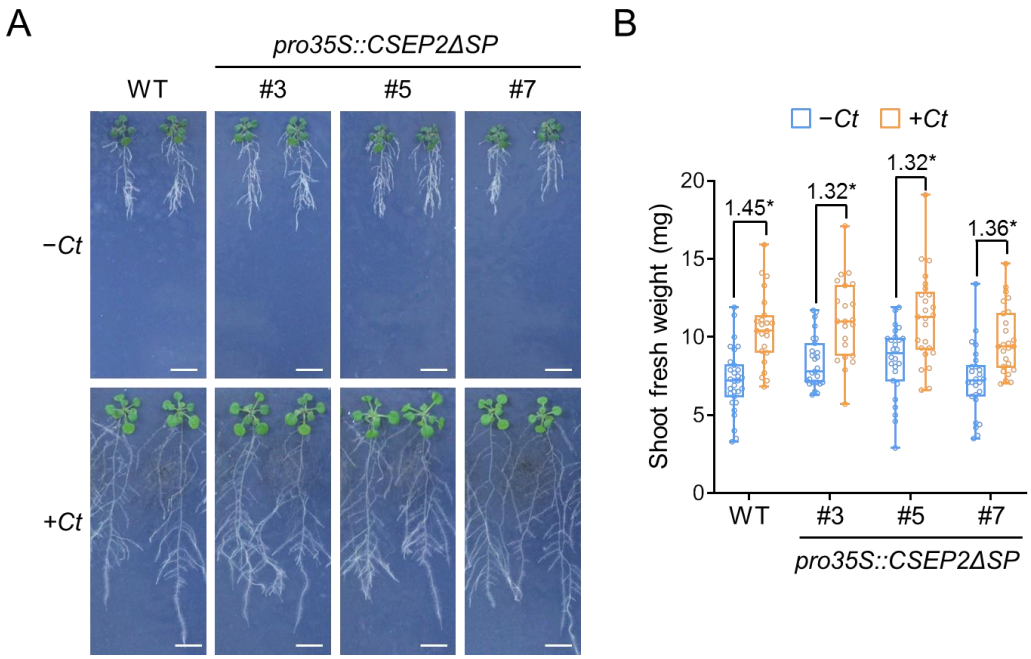

Figure 28. *Ct*-mediated plant growth promotion is retained in *CSEP2*-expressing plants.
(A) A representative image of WT and *pro35S::CSEP2ΔSP* transgenic plants growth under low Pi conditions (50 μM) with and without *Ct* inoculation for 24 d. Two independent experiments were conducted. Scale bars indicate 1 cm.
(B) Quantitative analysis of shoot fresh weight (SFW) in WT and *pro35S::CSEP2ΔSP* transgenic plants under low Pi conditions. SFW was determined at 24 dpi. N = 22-30. Two-tailed t-test was conducted to evaluate significantly differences between *Ct*-inoculated and uninoculated plants (calculated as SFW + *Ct*/- *Ct*, *p < 0.001).

CSEP2 alone was not sufficient to impair *Ct*-mediated plant growth promotion (Figure 28) and *CSEP2* attenuated cell wall-based defense by interfering with IG metabolic pathway. It is thus conceivable that another branch(es) in Trp-derived plant metabolism also contributes to *Ct*-mediated plant growth promotion, and/or that another effector(s) suppressed by Trp-derived metabolites is required for *Ct* pathogenesis. 4MI3A and CAM application effectively suppresses *Ct* overgrowth in *cyp79B2 cyp79B3* (Figure 4), implying that the IG and CAM pathways both contribute to *Ct*-mediated plant growth promotion. To test this idea, I examined *Ct*-mediated plant growth promotion in the mutants lacking these two branches, *cyp81F2 cyp81F3* and *pad3*, which are unable to generate 4MI3A or CAM, respectively. *Ct*-mediated plant growth promotion was not affected in *cyp81F2 cyp81F3* or *pad3* plants (Figure 29). Notably however, *Ct*-mediated shoot growth promotion was impaired in *cyp81F2 cyp81F3 pad3* triple mutants, compared to WT (Figure 29). These suggest that the 4MI3A and CAM pathways both, redundantly contribute to *Ct*-mediated growth promotion.

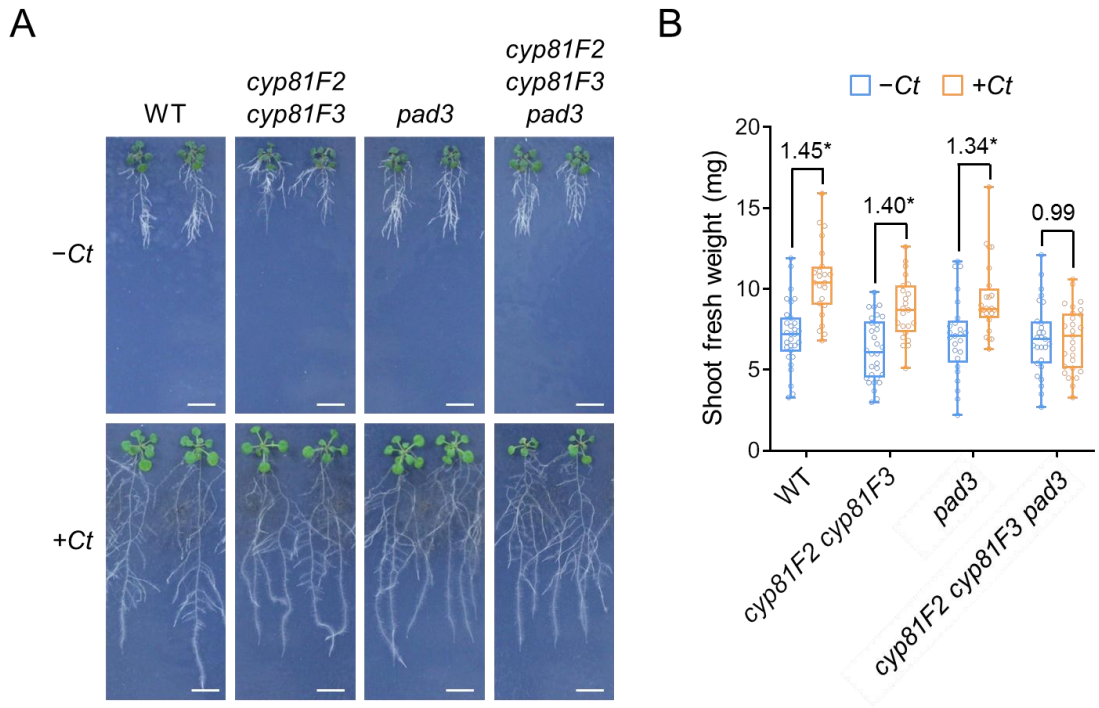

Figure 29. 4MI3A pathway and CAM pathway both contribute to *Ct*-mediated plant growth promotion.

(A) A representative image of WT, *cyp81F2 cyp81F3*, *pad3* and *cyp81F2 cyp81F3 pad3* plants under low Pi conditions (50 μM) with and without *Ct* inoculation for 24 d. Two independent experiments were conducted. Scale bars indicate 1 cm.

(B) Quantitative analysis of shoot fresh weight (SFW) of WT *cyp81F2 cyp81F3*, *pad3* and *cyp81F2 cyp81F3 pad3* plants in low Pi conditions. SFW was determined at 24 dpi. N = 22-30. Two-tailed t-test was conducted to evaluate statistical differences between *Ct*-inoculated and uninoculated plants (calculated as SFW + *Ct*/- *Ct*, *p < 0.01).

DISCUSSION

In this study, I show that two *CSEPs* act as fungal infection-promoting factors in *Ct*, and that their expression is repressed during beneficial interactions by a subset of plant Trp-derived metabolites (Figure 10 and 14). This is consistent with previous studies that fungal overgrowth is associated with the loss of *Ct* benefits in *A. thaliana* mutants compromised in the host Trp metabolism (Hiruma et al., 2016). This work gains important insight into the mechanisms by which *Ct* expresses pathogenesis in the absence of host Trp-derived metabolites. Pathogens typically employ a wide array of effectors to suppress PTI for promoting infection (Cui et al., 2015; Irieda et al., 2019; Jones et al., 2006). This work demonstrates that endophytic fungi also have infection-promoting effectors, including *CSEP2* that attenuates MAMP-induced callose deposition. The significance of this defense suppression is underscored by increased *Ct* colonization when PTI-associated callose deposition is lost or reduced in *pmr4* or *CSEP2*-transgenic plants, respectively (Figures 10 and 27). Beneficial mycorrhizal fungi and rhizobia have also been reported to secrete effectors to counteract host PTI, thereby promoting colonization, to facilitate their symbiotic processes (Deakin et al., 2009; Plett et al., 2020; Voß et al., 2018; Zeng et al., 2020). Together with these studies, this study extends the view to non-mycorrhizal beneficial fungi that fungal infection is limited by host PTI, yet fungi have evolved effectors to counteract and overcome PTI.

This study for the first time reveals an effector in non-mycorrhizal beneficial fungi, *CtCSEP2*, which attenuates MAMP-induced callose deposition. This extends a repertoire of host targets in mutualistic microbes (Deakin et al., 2009; Plett et al., 2020; Voß et al., 2018; Zeng et al., 2020). Although effectors suppressing callose deposition have been described in different pathogen, e.g. through interfering with defense signaling within or proximal to the PRR complexes (Göhre et al., 2008; Hauck et al., 2003; Kim et al., 2005; Tomczynska et al., 2020; Wang et al., 2021), this study indicates the existence of a novel mechanism for callose inhibition by plant-infecting microbes, i.e. interfering with the host IG metabolism.

Trp-derived plant metabolites suppress fungal overgrowth during beneficial interactions with *Ct* in *A. thaliana*

Cruciferous plants including *A. thaliana* are characterized by family-specific evolution and diversification of antimicrobial metabolites derived from Trp, such as glucosinolates and their breakdown products, isothiocyanates, thiocyanates and nitriles (Halkier and Gershenzon, 2006). In particular, the IG biosynthesis pathway mediates broad-spectrum resistance against a wide range of plant pathogens (Bednarek et al., 2009).

The significance of these metabolites in beneficial *Ct* interactions is evident with the pathogenesis displayed by *Ct* in c*yp79B2 cyp79B3* plants, which are impaired at the initial,

critical step of Trp metabolism for producing IAOx (Hiruma et al., 2016). As IAOx provides a common precursor for multifurcating metabolic branches, it is important to elucidate what IAOx derivatives serve in suppressing potential *Ct* pathogenesis during beneficial interactions. Downstream of IAOx, the immunity function of IGs is dependent on *CYP81F2* P450 monooxygenase that hydroxylates I3G to produce 4OHI3G, a precursor for 4MI3G (Figure 1, Bednarek et al., 2009; Clay et al., 2009). This work has unveiled a significant increase in *Ct* growth at an early infection stage in *cyp81F2 cyp81F3* plants, but not in plants that are defective in downstream branches (Figure 7). It is possible that redundant myrosinases mediate 4MI3G hydrolysis. Notably, however, *CYP81F2* and *PEN2* both contribute to leaf resistance against different fungal pathogens such as *Blumeria graminis f.sp. hordei*, *Erysiphe pisi* and *Plectosphaerella cucumerina* (Bednarek et al., 2009). It has been also reported that *Ct* growth is increased in *pen2* at a late colonization stage, possibly under different inoculation conditions from ours (Frerigmann et al., 2020). Trp-derived diverse metabolites may differentially suppress fungal growth at different infection modes and/or steps. Determination of bioactive forms of these metabolites and precise understanding of their functions and regulations require further in-depth studies.

This work shows that an as-yet-undetected IG metabolite 4MI3A, presumably derived from PEN2-mediated hydrolysis of 4MI3G, inhibits *Ct* growth specifically *in planta*. The failure for 4MI3A to inhibit fungal growth *in vitro* implies that 4MI3A suppression of *Ct* overgrowth is dependent on its conversion to an active anti-microbial compound(s) or its stimulation of plant immunity. My data suggest that at least some Trp-derived metabolites serve to strengthen MAMP-induced callose deposition against its perturbation during fungal infection. Therefore, Trp-derived metabolites seem to suppress fungal growth in roots not only as antimicrobial compounds but also at least through the reinforcement of cell wall-based defense, thereby contributing to beneficial interactions with *Ct*.

In this study, the effects of Trp-derived metabolites on *Ct* fungal growth and plant growth promotion were tested under low Pi conditions. However, Pi levels also affect the infection modes of *Ct*. *Ct* promotes plant growth only under Pi-deficient conditions, but not under Pi-sufficient conditions (Hiruma et al., 2016)), implying that, in addition to Trp-derived metabolies, phosphate status plays a role in the transition from pathogenic to beneficial lifestyles. Transcriptome analyses on Pi-depleted and Pi-supplied roots in response to *Ct* indicate a greater activation of ‘defense response’ and ‘indole glucosinolate metabolic processes’ in *Ct*-colonized roots under Pi-sufficient compared to Pi-deficient conditions (Hacquard et al., 2016). Further studies on Trp-derived plant metabolites controlling fungal growth under Pi-sufficient conditions is also valuable for exploring the molecular basis for the Pi status dependence and its possible links to Trp metabolism in *Ct*-plant interactions.

Ct CSEPs promote fungal colonization in *A. thaliana* roots

Plant pathogens have typically adapted their infection-promoting strategies and effectors to the host plants (Alfano et al., 2004; De Wit et al., 2009; Kamoun, 2006; Rehman et al., 2016). This study has exploited the root endophyte and pathogen models *Ct* and *Ci*, respectively, which are closely related to each other (Hacquard et al., 2016), to compare and investigate into the molecular mechanisms underlying their contrasting infection modes. A smaller repertoire of *CSEP* genes in *Ct* compared to *Ci*, at both the genome and transcriptome levels (Hacquard et al., 2016), suggests that restriction of *CSEP* activities is a key to establish beneficial interactions with endophytic fungi. Indeed, endophytic *Ct* turns to be a pathogen in *cyp79B2 cyp79B3* plants, in which fungal virulence is de-repressed in the absence of Trp-derived metabolites (Hiruma, et al., 2016). A comparative fungal transcriptome analysis has revealed 11 *CSEPs*, which were highly induced during colonization in *cyp79B2 cyp79B3* plants compared to WT (Figure 8). Here I pursued the hypothesis that these *CSEPs* facilitate *Ct* growth and/or its transition from beneficial to pathogenic infection modes. Of these *CSEPs*, two *CSEPs* promote *Ct* colonization when individually introduced as transgenes without SP sequences into *A. thaliana*. To test the physiological relevance of these findings, *Ct* mutants disrupted with and constitutively expressing these *CSEPs*, currently being generated, need to be examined in this context. Nevertheless, my results indicate that two *CSEPs* have the ability to promote *Ct* infection through some functions in the host cytoplasm.

CSEP2 homologs are widely distributed within the *Colletotrichum* genus. Interestingly, *Colletotrichum* species, carrying *Ct CSEP2* homologs of high similarity, such as *C. incanum*, *C. higginsianum* and *C. shisoi*, ranging from 78.3% to 60% (Table 1), as well as *C. tofieldiae*, colonize *Brassicaceae* plants. The IG biosynthesis pathway emanating from Trp has evolved and diversified extensively in Brassicales. These *CSEP2* homologs in the *Brassicaceae* -adapted *Colletotrichum* species, may play a common role in promoting fungal infection against IG-mediated host defense characteristic of *Brassicaceae* plants. It is conceivable that attenuation of *PMR4*-medaited cell wall-based defense is a conserved function for *CSEP2* homologs. Motif-domain searching program, including InterPro and PROSITE, have not revealed discernible functional domains or motifs in *CSEP2* protein sequences, as is usual with microbial effectors. The mechanisms by which *Ct-CSEP2* attenuates callose deposition and whether it also has another host target(s) require further investigation.

Notably, *CSEP2* expression is silenced in *Ct* during beneficial interactions, whereas it is induced during pathogenesis in the absence of host Trp metabolism. It is important to explore the molecular basis for differential *CSEP* expression between endophytic and pathogenic infection modes in *Colletotrichum* species. This regulation seems in contrast to the aforementioned defense-attenuating effectors in mycorrhizal fungi and symbiotic bacteria, which are expressed to promote colonization and symbiosis. Whether their effector over-activation leads to pathogenesis, and if so how it is prevented during symbioses,

represents an interesting topic for future studies.

CSEP2 suppresses MAMP-triggered callose deposition dependent on IGs

CSEP2 conserved in *Colletotrichum* species, but not *Ct*-specific *CSEP9*, specifically suppresses MAMP-induced callose deposition. In leaves, the loss of *PMR4* callose synthase leads to enhanced fungal resistance in an SA dependent manner (Nishimura et al., 2003). By contrast, *PMR4*-dependent callose deposition contributes to flg22-induced resistance against *hrcC* mutant strain of the bacterial pathogen *Pseudomomas syringae* DC3000, which lacks T3SS delivering virulence effectors into the host cell (Kim et al., 2005). These findings suggest that *PMR4* contributes to PTI, and that its loss leads to enhanced immunity in leaves in the presence of pathogen effectors, presumably via ETI-like backup resistance mounted on effector recognition. Enhanced *Ct* growth in *pmr4* (Figure 27) indeed points to a critical role for callose deposition in limiting *Ct* colonization.

It is thus remarkable that the suppression of callose deposition by *CSEP2* or *pmr4* is not accompanied by backup resistance in roots (Figures 17 and 10). This can be explained by the scarcity of effector expression during beneficial interactions with *Ct*, which is reminiscent of the aforementioned T3SS-deficient bacteria.

Ci also infects *pmr4* roots without encountering strong resistance, despite extensive induction of callose deposition at the cell wall papillae (Figure 26 and Figure 27). In the case of *Ci*, loss of *PMR4*-dependent callose deposition does not further increase fungal growth or lead to backup resistance activation. This may be attributed to effective suppression of callose deposition and/or backup resistance activation, enabled by a rich repertoire of *CSEP*-encoding effectors expressed in *Ci*. It is also conceivable that the lack of chloroplasts hampers active SA biosynthesis and backup resistance activation upon fungal perturbation of callose deposition in roots.

Despite the evident requirement for the IG pathway in MAMP-induced callose deposition (Clay et al., 2009; Millet et al., 2010), the mechanisms by which IG derivatives including 4MI3A regulate callose deposition are still obscure. Detecting and tracing 4MI3A with an isotope label *in planta* may help identify a bioactive form(s) toward the elucidation of how it regulates callose deposition. In this context, *Ct CSEP2* may provide a useful probe to reveal an "Achilles heel" in the host defense regulation. Screening for CtCSEP2 interacting plant proteins may help reveal a critical step in the plant-fungus competition over the Trp metabolic pathway.

Trp-derived plant metabolites control *Ct* infection in various ways during beneficial interactions

Ct CSEP2 is likely to interfere with some steps in the 4MI3A branch to attenuate callose deposition, thereby promoting fungal growth, but *Ct*-mediated plant growth promotion under

low Pi conditions is not affected in transgenic plants overexpressing *CtCSEP2* (Figure 28). In *pmr4*, suppression of MAMP-induced callose deposition is associated with increased *Ct* growth (Figure 27) and also apparently with defects in *Ct*-mediated plant growth promotion (Preliminary data not shown). This may be correlated with possible differences in fungal growth and/or behavior between the two host genotypes. It is important to determine a threshold for fungal growth levels, beyond which *Ct* growth negatively influences plant growth, and what is needed in addition to *CSEP2* for *Ct* to exceed this threshold.

In the absence of 4MI3A or camalexin in *cyp81F2 cyp81F3* and *pad3* mutants, respectively, *Ct* also displays WT-like plant growth promotion (Figure 29). MAMP-induced callose deposition is reduced in *cyp81F2 cyp81F3* (Figure 19) but is retained in *pad3* (Clay et al, Science 2009). Strikingly however, the simultaneous disruption of the two pathways results in the loss of *Ct*-mediated plant growth promotion in *cyp81F2 cyp81F3 pad3*, albeit without discernible disease symptoms (Figure 29). This suggests that an array of Trp-derived metabolites collectively contribute to the proper control of *Ct* growth and benefits, possibly in callose-dependent and -independent manners. The obvious differences in *Ct* infection modes and *Ct* effects on plant growth between *cyp81F2 cyp81F3 pad3* and *cyp79B2 cyp79B3* plants (Figure 29; Hiruma et al., 2016) imply the existence of another Trp-derived metabolite(s) controlling *Ct* growth and plant growth promotion, which is largely retained in the former mutant but lost in the latter mutant. The precise mechanisms by which these metabolites influence *Ct* infection modes and growth require further exploration, but the present data point to the existence of various roles played by different Trp-derived plant metabolites (Figure 30).

My findings suggest that *Ct* growth is restricted by *Ct*-induced callose-rich papillae at fungal contact sites, and that *Ct* has *CSEP2*, if expressed, which can effectively attenuate MAMP-induced callose deposition. Importantly, the host employs a subset of Trp metabolites not only to repress *CSEP2* expression but also to counteract its callose-suppressing function, indicated by the restoration of flg22-induced callose deposition in *pro35S::CSEP2ΔSP* plants with 4MI3A (Figure 20). My study has discovered a competition between effector-mediated suppression and Trp metabolite-mediated reinforcement of cell wall-based defense, which plays a critical role in fungal growth control during plant interactions with beneficial endophytes.

Conclusions

Currently, many pathogen effectors have been reported to promote host infection of the pathogen. However, the colonization strategies of endophytes, and host control of their colonization during beneficial interactions are still largely unknown. I revealed an infection promoting effector, *CSEP2*, in the root endophytic fungus *Ct*, which possibly interferes with some steps in the IG pathway to attenuate cell wall-based defense conferred by

MAMP-induced callose deposition, thereby promoting *Ct* infection. Host Trp-derived metabolites suppress *CSEP2* expression and function, thereby strengthening MAMP-induced callose deposition, to counteract *Ct* infection strategies. A competition between fungal effectors and host Trp metabolism over MAMP-induced callose deposition provides a critical step in beneficial plant-fungus interactions.

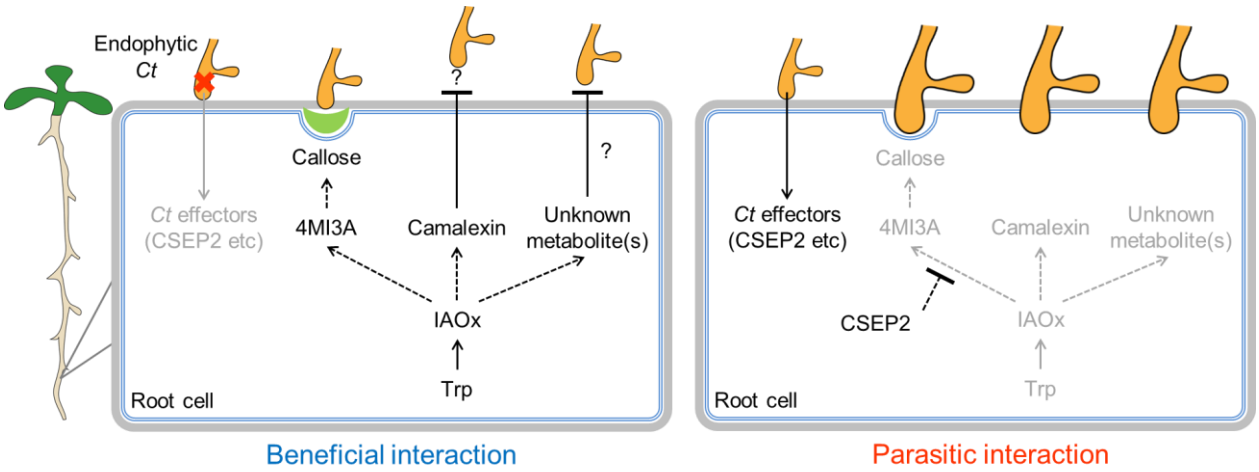

Figure 30. A competition between fungal effectors and host tryptophan metabolism controls interactions with endophytic fungi in *A. thaliana*.

The endophytic fungus *Ct* secretes infection-promoting effectors, such as *CSEP2*, into the cytoplasm of root cells during colonization in *A. thaliana*. In WT plants, a subset of Trp-derived metabolites suppresses *CSEP2* expression, while IG-dependent MAMP-induced callose deposition at fungal penetration sites in the plant cell wall restricted *Ct* invasion. Studies on *CSEP2*-expressing transgenic plants or Trp metabolism-deficient mutants point to a model in which *CSEP2*, if expressed, can interfere with certain step(s) upstream of 4MI3A but downstream of I3G in the IG pathway to attenuate MAMP-induced callose deposition, thereby promoting *Ct* infection. Exogenous application of 4MI3A strengthens MAMP-induced callose deposition, and thereby counteracts *CSEP2*-mediated callose-suppression. In addition, camalexin and some unknown metabolite(s) also contribute to suppressing *Ct* overgrowth and pathogenesis, likely through a mechanism(s) different than callose deposition, during beneficial interactions.

ACKNOWLEDGEMENT

My deepest gratitude goes first and foremost to Professor Yusuke Saijo, my supervisor, for his constant encouragement and guidance. With his illuminating instruction and useful suggestions throughout the undertaking of this study, greatly help me to writing this thesis. Second, I would like to express my heartfelt gratitude to Professor Kei Hiruma, who led me from the beginning and spent numerous hours for all of three past years. Without his instructive advice, impressive kindness and patience, this thesis would not have been able to be finished smoothly.

I would like to thank my thesis committee members, Professor Keiji Nakajima and Professor Takayuki Tohge, for all of their insightful comments and discussions through this process.

I am also thankful for Dr. Shigetaka Yasuda provided all the experimental advice, ideas and discussion, which would be absolutely invaluable.

I gratefully acknowledge Kazuki Tsurukawa, the member of Plant Immunity laboratory, who greatly made effort to this study.

I would like to take this opportunity to thank our collaborators, Dr. Yoshiaki Nakao and Dr. Semba Kazuhiko from Kyoto University, Dr. Mutsumi Watanabe from Plant Secondary Metabolism laboratory in NAIST, Dr. Keisuke Tanaka from NODAI Genome Research Center in Tokyo University of Agriculture, and Dr. Teruaki Taji from the University of Tokyo. All of them assisted for the process of this study.

Thanks to technical support staff Uchiyama Akemi and Matsubara Mie for their greatly help.

My thanks also go to those colleagues in the laboratory of Plant Immunity and NAIST staffs, for their assistance in producing this thesis.

Thanks to the MEXT scholarship for supporting my studies and life in Japan.

Finally, I would like to thank my beloved family, friends, especially my spouse, for their loving considerations, intimate company, and spiritual support all through these years.

Thanks to all members helped me!

REFERENCES

Agerbirk, N., De Vos, M., Kim, J.H., & Jander, G. (2009). Indole glucosinolate breakdown and its biological effects. *Phytochemistry Reviews*, 8(1), 101.

Aist, J.R. (1976). Papillae and related wound plugs of plant cells. *Annual Review of Phytopathology*, 14(1), 145-163.

Aist, J.R., Bushnell, W.R. (1991). Invasion of plants by powdery mildew fungi, and cellular mechanisms of resistance. In The Fungal Spore and Disease Initiation in Plants and Animals, G.T. Cole, and H.C. Mock, eds (New York: Plenum), pp. 321-345.

Alfano, J.R., Collmer, A. (2004). Type III secretion system effector proteins: double agents in bacterial disease and plant defense. *Annu. Rev. Phytopathol.*, 42, 385-414.

Antoun, H. (2012). Beneficial microorganisms for the sustainable use of phosphates in agriculture. *Procedia Engineering*, 46, 62-67.

Bednarek, P., Piślewska-Bednarek, M., Svatoš, A., Schneider, B., Doubský, J., Mansurova, M., Molina, A. (2009). A glucosinolate metabolism pathway in living plant cells mediates broad-spectrum antifungal defense. *Science*, 323(5910), 101-106.

Bednarek, P., Piślewska-Bednarek, M., Ver Loren van Themaat, E., Maddula, R.K., Svatoš, A., Schulze-Lefert, P. (2011). Conservation and clade-specific diversification of pathogen-inducible tryptophan and indole glucosinolate metabolism in Arabidopsis thaliana relatives. *New Phytologist*, 192(3), 713-726.

Binyamin, R., Nadeem, S.M., Akhtar, S., Khan, M.Y., Anjum, R. (2019). Beneficial and pathogenic plant-microbe interactions: A review. *Soil & Environment*, 38(2), 11-33.

Bohinc, T., Ban, G.S., Ban, D., Trdan, S. (2012). Glucosinolates in plant protection strategies: a review. *Archives of biological sciences*, 64(3), 821-828.

Boller, T., Felix, G. 2009. A renaissance of elicitors: perception of microbe-associated molecular patterns and danger signals by pattern-recognition receptors. *The Annual Review of Plant Biology*, 60, 379-406.

Bonfante, P., and Genre, A. (2010). Mechanisms underlying beneficial plant fungus interactions in mycorrhizal symbiosis. *Nature Communications*, 1, 48.

Cai, L., Hyde, K.D., Taylor, P.W. J., Weir, B., Waller, J., Abang, M.M., Prihastuti, H. (2009). A polyphasic approach for studying *Colletotrichum*. *Fungal Diversity*, 39(1), 183-204.

Cannon, P.F., Damm, U., Johnston, P.R., Weir, B.S. (2012). *Colletotrichum*-current status and future directions. *Studies in mycology*, 73, 181-213.

Clay N.K., Adio A.M., Denoux C., Jander G., Ausube F.M. (2009). Glucosinolate metabolites required for an Arabidopsis innate immune response. *Science*, 323: 95-101.

Cook, D.E., Mesarich, C.H., Thomma, B.P.H.J. (2015). Understanding plant Immunity as a surveillance system to detect invasion. *Annual review of Phytopathology*, 53, 541-563.

Cui, H., Tsuda, K., Parker, J.E. (2015). Effector-triggered immunity: from pathogen

perception to robust defense. *Annual review of plant biology*, 66, 487-511.

De Wit, P.J., Mehrabi, R., Van den Burg, H.A., Stergiopoulos, I. (2009). Fungal effector proteins: past, present and future. *Molecular plant pathology*, 10(6), 735-747.

Deakin, W.J., Broughton, W.J. (2009). Symbiotic use of pathogenic strategies: rhizobial protein secretion systems. *Nature Reviews Microbiology*, 7(4), 312-320.

Di, X., Cao, L., Hughes, R.K., Tintor, N., Banfield, M.J., Takken, F.L.W. (2017). Structure-function analysis of the Fusarium oxysporum Avr2 effector allows uncoupling of its immune-suppressing activity from recognition. *New Phytologist*, 216, 897-914.

Díaz-González, S., Marín, P., Sánchez, R., Arribas, C., Kruse, J., González-Melendi, P., Sacristán, S. (2020). Mutualistic fungal endophyte *Colletotrichum tofieldiae* Ct0861 colonizes and increases growth and yield of maize and tomato plants. *Agronomy*, 10(10), 1493.

Dixon, R.A. (2001). Natural products and plant disease resistance. *Nature*, 411(6839), 843-847.

Dou D., Zhou J.M. (2012). Phytopathogen effectors subverting host immunity: different foes, similar battleground. *Cell Host & Microbe*, 12, 484-495.

Ellinger, D., Naumann, M., Falter, C., Zwikowics, C., Jamrow, T., Manisseri, C., Voigt, C. A. (2013). Elevated early callose deposition results in complete penetration resistance to powdery mildew in Arabidopsis. *Plant physiology*, 161(3), 1433-1444.

Fahey, J. W., Zalcmann, A. T., Talalay, P. (2001). The chemical diversity and distribution of glucosinolates and isothiocyanates among plants. *Phytochemistry*, 56(1), 5-51.

Felix, G., Duran, J.D., Volko, S., Boller, T. (1999). Plants have a sensitive perception system for the most conserved domain of bacterial flagellin. *The Plant Journal*, 18(3), 265-276.

Felix, G., Regenass, M., Boller, T. (1993). Specific perception of subnanomolar concentrations of chitin fragments by tomato cells: induction of extracellular alkalinization, changes in protein phosphorylation, and establishment of a refractory state. *The Plant Journal*, 4(2), 307-316.

Frerigmann, H., Piotrowski, M., Lemke, R., Bednarek, P., Schulze-Lefert, P. (2021). A network of phosphate starvation and immune-related signaling and metabolic pathways controls the interaction between *Arabidopsis thaliana* and the beneficial fungus *Colletotrichum tofieldiae*. *Molecular Plant-Microbe Interactions*, MPMI-08.

Gan, P., Tsushima, A., Hiroyama, R., Narusaka, M., Takano, Y., Narusaka, Y., Shirasu, K. (2019). *Colletotrichum shisoi sp*. nov., an anthracnose pathogen of *Perilla frutescens* in Japan: molecular phylogenetic, morphological and genomic evidence. *Scientific reports*, 9(1), 1-13.

Glawischnig, E. (2007). Camalexin. *Phytochemistry*, 68(4), 401-406.

Glawischnig, E., Hansen, B.G., Olsen, C.E., Halkier, B.A. (2004). Camalexin is synthesized from indole-3-acetaldoxime, a key branching point between primary and secondary metabolism in Arabidopsis. *Proceedings of the National Academy of Sciences*, 101(21),

8245-8250.

Glawischnig, E., Hansen, B.G., Olsen, C.E., Halkier, B.A. (2004). Camalexin is synthesized from indole-3-acetaldoxime, a key branching point between primary and secondary metabolism in Arabidopsis. *Proceedings of the National Academy of Sciences*, 101(21), 8245-8250.

Göhre, V and Robatzek, S. (2008). Breaking the barriers: microbial effector molecules subvert plant immunity. *Annu. Rev. Phytopathol*., 46, 189-215.

Gómez-Gómez L., Boller T. (2000). FLS2: An LRR receptor-like kinase involved in the perception of the bacterial elicitor flagellin in Arabidopsis. *Molecular cell*, 5, 1003-11.

Grant, S.R., Fisher, E.J., Chang, J.H., Mole, B.M., Dangl, J.L. (2006). Subterfuge and manipulation: type III effector proteins of phytopathogenic bacteria. *Annu. Rev. Microbiol.*, 60, 425-449.

Habte, M. (2006). The roles of arbuscular mycorrhizas in plant and soil health. *Biological approaches to sustainable soil systems*, 129-147.

Hacquard, S., Kracher, B., Hiruma, K., Münch, P.C., Garrido-Oter, R., Thon, M.R., Weimann A., O'Connell, R.J. (2016). Survival trade-offs in plant roots during colonization by closely related beneficial and pathogenic fungi. *Nature Communications*, 7, 11362.

Hacquard, S., Spaepen, S., Garrido-Oter, R., Schulze-Lefert, P. (2017). Interplay between innate immunity and the plant microbiota. *Annual review of Phytopathology*, 55, 565-589.

Hagemeier, J., Schneider, B., Oldham, N.J., Hahlbrock, K. (2001). Accumulation of soluble and wall-bound indolic metabolites in *Arabidopsis thaliana* leaves infected with virulent or avirulent *Pseudomonas syringae* pathovar tomato strains. *Proceedings of the National Academy of Sciences*, 98(2), 753-758.

Halkier, B.A., Gershenzon, J. (2006). Biology and biochemistry of glucosinolates. *Annu. Rev. Plant Biol.*, 57, 303-333.

Hauck, P., Thilmony, R., He, S.Y. (2003). A *Pseudomonas syringae* type III effector suppresses cell wall-based extracellular defense in susceptible *Arabidopsis* plants. *Proceedings of the National Academy of Sciences*, 100(14), 8577-8582.

Hiruma, K. (2019). Roles of plant-derived secondary metabolites during interactions with pathogenic and beneficial microbes under conditions of environmental stress. *Microorganisms*, 7(9), 362.

Hiruma, K., Fukunaga, S., Bednarek, P., Piślewska-Bednarek, M., Watanabe, S., Narusaka, Y., Takano, Y. (2013). Glutathione and tryptophan metabolism are required for Arabidopsis immunity during the hypersensitive response to hemibiotrophs. *Proceedings of the National Academy of Sciences*, 110(23), 9589-9594.

Hiruma, K., Gerlach, N., Sacristán, S., Nakano, R.T., Hacquard, S., Kracher, B., Schulze-Lefert, P. (2016). Root Endophyte *Colletotrichum tofieldiae* confers plant fitness benefits that are phosphate status dependent. *Cell*, 165(2), 464-474.

Hiruma, K., Kobae, Y., Toju, H. (2018). Beneficial associations between Brassicaceae plants and fungal endophytes under nutrient-limiting conditions: evolutionary origins and host-symbiont molecular mechanisms. *Current Opinion in Plant Biology*, 44, 145-154.

Hiruma, K., Onozawa-Komori, M., Takahashi, F., Asakura, M., Bednarek, P., Okuno, T., Takano, Y. (2010). Entry Mode-Dependent Function of an Indole Glucosinolate Pathway in Arabidopsis for Nonhost Resistance against Anthracnose Pathogens. *The Plant Cell*, 22(7), 2429-2443.

Irieda, H., Inoue, Y., Mori, M., Yamada, K., Oshikawa, Y., Saitoh, H., Uemura, A., Terauchi, R., Kitakura, S., Kosaka, A. (2019). Conserved fungal effector suppresses PAMP-triggered immunity by targeting plant immune kinases. *PNAS*, 116, 496-505.

Jayawardena, R.S., Hyde, K.D., Damm, U., Cai, L., Liu, M., Li, X. H., Yan, J. Y. (2016). Notes on currently accepted species of *Colletotrichum*. *Mycosphere*, 7, 1192-1260.

Jones, J.D.G, and Dangl, J.L. (2006). The plant immune system. *Nature*, 444, 323-329.

Kamoun, S. (2006). A catalogue of the effector secretome of plant pathogenic oomycetes. *Annual review of phytopathology*, 44.

Khodadadi, F., González, J.B., Martin, P.L., Giroux, E., Bilodeau, G.J., Peter, K. A., Aćimović, S.G. (2020). Identification and characterization of *Colletotrichum* species causing apple bitter rot in New York and description of *C. noveboracense* sp. nov. *Scientific reports*, 10(1), 1-19.

Kim, M.G., Da Cunha, L., McFall, A.J., Belkhadir, Y., DebRoy, S., Dangl, J.L., Mackey, D. (2005). Two *Pseudomonas syringae* type III effectors inhibit RIN4-regulated basal defense in *Arabidopsis*. *Cell*, 121(5), 749-759.

Kliebenstein, D. J., Rowe, H.C., Denby, K.J. (2005). Secondary metabolites influence Arabidopsis/Botrytis interactions: variation in host production and pathogen sensitivity. *The Plant Journal*, 44, 25-36.

Lahrmann, U., Strehmel, N., Langen, G., Frerigmann, H., Leson, L., Ding, Y., Zuccaro, A. (2015). Mutualistic root endophytism is not associated with the reduction of saprotrophic traits and requires a noncompromised plant innate immunity. *New Phytologist*, 207(3), 841-857.

Lipka, V., Dittgen, J., Bednarek, P., Bhat R., Wiermer, M., Stein, M., Landtag, J., Brandt, W. (2005). Pre- and postinvasion defenses both contribute to nonhost resistance in Arabidopsis. *Science*, 310(5751), 1180-1183.

Luna, E., Pastor, V., Robert, J., Flors, V., Mauch-Mani, B., Ton, J. (2011). Callose deposition: a multifaceted plant defense response. *Molecular Plant-Microbe Interactions*, 24(2), 183-193.

Lynch, J.P. (2011). Root phenes for enhanced soil exploration and phosphorus acquisition: tools for future crops. Plant physiology, 156(3), 1041-1049.

Manjunath, A., Hue, N.V., Habte, M. (1989). Response of *Leucaena leucocephala* to vesicular-arbuscular mycorrhizal colonization and rock phosphate fertilization in an

Oxisol. *Plant and soil*, 114(1), 127-133.

Meyer, A., Pühler, A., Niehaus, K. (2001). The lipopolysaccharides of the phytopathogen *Xanthomonas campestris pv. campestris* induce an oxidative burst reaction in cell cultures of *Nicotiana tabacum*. *Planta*, 213(2), 214-222.

Meyer, D., Pajonk, S., Micali, C., O'Connell, R., Schulze-Lefert, P. (2009). Extracellular transport and integration of plant secretory proteins into pathogen-induced cell wall compartments. *The Plant Journal*, 57(6), 986-999.

Millet, Y.A., Danna, C.H., Clay, N.K., Songnuan, W., Simon, M.D., Werck-Reichhart, D., Ausubel, F.M. (2010). Innate immune responses activated in Arabidopsis roots by microbe-associated molecular patterns. *The Plant Cell*, 22(3), 973-990.

Miya, A., Albert, P., Shinya, T., Desaki, Y., Ichimura, K., Shirasu, K., Shibuya, N. (2007). CERK1, a LysM receptor kinase, is essential for chitin elicitor signaling in Arabidopsis. *Proceedings of the National Academy of Sciences*, 104(49), 19613-19618.

Morcillo, R.J., Singh, S.K., He, D., An, G., Vílchez, J.I., Tang, K., Yang, Y. (2020). Rhizobacterium-derived diacetyl modulates plant immunity in a phosphate-dependent manner. *The EMBO journal*, 39(2), e102602.

Nishimura, M.T., Stein, M., Hou, B.H., Vogel, J.P., Edwards, H., Somerville, S.C. (2003). Loss of a callose synthase results in salicylic acid-dependent disease resistance. *Science*, 301(5635), 969-972.

Nongbri, P.L., Johnson, J.M., Sherameti, I., Glawischnig, E., Halkier, B.A., Oelmüller, R. (2012). Indole-3-acetaldoxime-derived compounds restrict root colonization in the beneficial interaction between Arabidopsis roots and the endophyte Piriformospora indica. *Molecular Plant-Microbe Interactions*, 25(9), 1186-1197.

Pastorczyk, M., Bednarek, P. (2016). The function of glucosinolates and related metabolites in plant innate immunity. In Advances in botanical research, Kopriva S, ed. (London, UK: Academic Press/Elsevier Science), pp. 171-198.

Pastorczyk, M., Kosaka, A., Piślewska-Bednarek, M., López, G., Frerigmann, H., Kułak, K., Bednarek, P. (2020). The role of CYP71A12 monooxygenase in pathogen-triggered tryptophan metabolism and Arabidopsis immunity. *New Phytologist*, 225(1), 400-412.

Pfalz, M., Mikkelsen, M.D., Bednarek, P., Olsen, C.E., Halkier, B.A., Kroymann, J. (2011). Metabolic engineering in Nicotiana benthamiana reveals key enzyme functions in Arabidopsis indole glucosinolate modification. *The Plant Cell*, 23(2), 716-729.

Pfalz, M., Vogel, H., Kroymann, J. (2009). The gene controlling the *indole glucosinolate modifier1* quantitative trait locus alters indole glucosinolate structures and aphid resistance in Arabidopsis. *The Plant Cell*, 21(3), 985-999.

Plett, J.M., Plett, K.L., Wong-Bajracharya, J., de Freitas Pereira, M., Costa, M.D., Kohler, A., Anderson, I.C. (2020). Mycorrhizal effector PaMiSSP10b alters polyamine biosynthesis in *Eucalyptus* root cells and promotes root colonization. *New Phytologist*, 228(2), 712-727.

Presti, L.L., Lanver, D., Schweizer, G., Tanaka, S., Liang, L., Tollot, M., Zuccaro, A., Reissmann, S., Kahmann, R. (2015). Fungal effectors and plant susceptibility. *Annual Review of Plant Biology*, 66, 513-45.

Rajniak, J., Barco, B., Clay, N.K., Sattely, E.S. (2015). A new cyanogenic metabolite in *Arabidopsis* required for inducible pathogen defence. *Nature*, 525(7569), 376-379.

Rehman, S., Gupta, V.K., Goyal, A.K. (2016). Identification and functional analysis of secreted effectors from phytoparasitic nematodes. *BMC microbiology*, 16(1), 48.

Rogers, E.E., Glazebrook, J., Ausubel, F.M. (1996). Mode of action of the Arabidopsis thaliana phytoalexin camalexin and its role in *Arabidopsis*-pathogen interactions. *Molecular Plant Microbe Interactions*. 9, 748-757.

Rojas, C.M., Senthil-Kumar, M., Tzin, V., Mysore, K. (2014). Regulation of primary plant metabolism during plant-pathogen interactions and its contribution to plant defense. *Frontiers in plant science*, 5, 17.

Saijo, Y., Loo, E.P.I., Yasuda, S. (2018). Pattern recognition receptors and signaling in plant-microbe interactions. *The Plant Journal*, 93(4), 592-613.

Sanchez-Vallet, A., Ramos, B., Bednarek, P., López, G., Piślewska-Bednarek, M., Schulze-Lefert, P., Molina, A. (2010). Tryptophan-derived secondary metabolites in Arabidopsis thaliana confer non-host resistance to necrotrophic *Plectosphaerella cucumerina* fungi. *The Plant Journal*. 63(1), 115-127.

Schlaeppi, K., Abou-Mansour, E., Buchala, A., Mauch, F. (2010). Disease resistance of Arabidopsis to Phytophthora brassicae is established by the sequential action of indole glucosinolates and camalexin. *The Plant Journal*, 62(5), 840-851.

Schmidt, S.M., Houterman, P.M., Schreiver, I., Ma, L., Amyotte, S., Chellappan, B., Boeren, S., Takken, F.L.W., Rep, M. (2013). MITEs in the promoters of effector genes allow prediction of novel virulence genes in *Fusarium oxysporum*. *BMC Genomics*, 14, 119.

Schuhegger, R., Nafisi, M., Mansourova, M., Petersen, B.L., Olsen, C.E., Svatoš, A., Glawischnig, E. (2006). CYP71B15 (PAD3) catalyzes the final step in camalexin biosynthesis. *Plant physiology*, 141(4), 1248-1254.

Sellam, A., Iacomi-Vasilescu, B., Hudhomme, P., Simoneau, P. (2007). *In vitro* antifungal activity of brassinin, camalexin and two isothiocyanates against the crucifer pathogens *Alternaria brassicicola* and *Alternaria brassicae*. *Plant Pathology*. 56, 296-301.

Shinya, T., Nakagawa, T., Kaku, H., Shibuya, N. 2015. Chitin-mediated plant-fungal interactions: catching, hiding and handshaking. *Current Opinion in Plant Biology*, 26, 64-71.

Tintor, N., Paauw, M., Rep, M., Takken, F.L.W. (2020). The root-invading pathogen Fusarium oxysporum targets pattern-triggered immunity using both cytoplasmic and apoplastic effectors. *New Phytologist*, 227(5), 1479-1492.

Tomczynska, I., Stumpe, M., Doan, T.G., Mauch, F. (2020). A Phytophthora effector protein promotes symplastic cell-to-cell trafficking by physical interaction with

plasmodesmata-localised callose synthases. *New Phytologist*, 227(5), 1467-1478.

Vogel, J., Somerville, S. (2000). Isolation and characterization of powdery mildew-resistant *Arabidopsis* mutants. *Proceedings of the National Academy of Sciences*, 97(4), 1897-1902.

Vosátka, M., Albrechtová, J. (2009). Benefits of Arbuscular Mycorrhizal Fungi to Sustainable Crop Production. In Microbial Strategies for Crop Improvement, Khan M., Zaidi A., Musarrat J. ed, pp. 205-225.

Voß, S., Betz, R., Heidt, S., Corradi, N., Requena, N. (2018). RiCRN1, a crinkler effector from the arbuscular mycorrhizal fungus *Rhizophagus irregularis*, functions in arbuscule development. *Frontiers in microbiology*, 9, 2068.

Wang, D., Tian, L., Zhang, D.D., Song, J., Song, S.S., Yin, C.M., Zhou, L., Liu, Y., Wang, B.Y., Kong, Z.Q. (2020). Functional analyses of small secreted cysteine-rich proteins identified candidate effectors in *Verticillium dahlia*. *Molecular Plant Pathology*, 21(5), 667-685.

Wang, W., Yang, J., Zhang,J., Bai, Y., Lei, X.G., Zhou, J.M. (2020). An Arabidopsis secondary metabolite directly targets expression of the bacterial Type III secretion system to inhibit bacterial virulence. *Cell Host & Microbe*, 27, 601-613.

Wang, Y., Li, X., Fan, B., Zhu, C., Chen, Z. (2021). Regulation and Function of Defense-Related Callose Deposition in Plants. *International Journal of Molecular Sciences*, 22(5), 2393.

Wawra, S., Fesel, P., Widmer, H., Timm, M., Seibel, J., Leson, L., Kesseler, L., Nostadt, R., Hilbert, M., Langen, G. (2016). The fungal-specific beta-glucan-binding lectin FGB1 alters cell-wall composition and suppresses glucan-triggered immunity in plants. *Nature Communications*, 7, 13188.

Wildermuth, M.C., Dewdney, J., Wu, G., Ausubel, F.M. (2002). Corrigendum: Isochorismate synthase is required to synthesize salicylic acid for plant defence. *Nature*, 417(6888), 571-571.

Wu, Y., Wood, M.D., Tao, Y., Katagiri, F. (2003). Direct delivery of bacterial avirulence proteins into resistant Arabidopsis protoplasts leads to hypersensitive cell death. *The Plant Journal*, 33(1), 131-137.

Xu, J., Meng, J., Meng, X., Zhao, Y., Liu, J., Sun, T., Zhang, S. (2016). Pathogen-responsive MPK3 and MPK6 reprogram the biosynthesis of indole glucosinolates and their derivatives in Arabidopsis immunity. *The Plant Cell*, 28(5), 1144-1162.

Zaynab, M., Fatima, M., Abbas, S., Sharif, Y., Umair, M., Zafar, M.H., Bahadar, K. (2018). Role of secondary metabolites in plant defense against pathogens. *Microbial pathogenesis*, 124, 198-202.

Zeng, T., Rodriguez-Moreno, L., Mansurkhodzaev, A., Wang, P., van den Berg, W., Gasciolli, V., Limpens, E. (2020). A lysin motif effector subverts chitin-triggered immunity to facilitate arbuscular mycorrhizal symbiosis. *New Phytologist*, 225(1), 448-460.

Zhao, Y., Hull, A.K., Gupta, N.R., Goss, K.A., Alonso, J., Ecker, J.R., Normanly, J., Chory, J., Celenza, J.L. (2002). Trp-dependent auxin biosynthesis in Arabidopsis: involvement of cytochrome P450s CYP79B2 and CYP79B3. *Genes & Development*, 16(23), 3100-3112.

Zhou, N., Tootle, T.L., Glazebrook, J. (1999). Arabidopsis *PAD3*, a gene required for camalexin biosynthesis, encodes a putative cytochrome P450 monooxygenase. *The Plant Cell*, 11(12), 2419-2428.

Zipfel, C., Robatzek, S., Navarro, L., Oakeley, E.J., Jones, J.D., Felix, G., Boller, T. (2004). Bacterial disease resistance in *Arabidopsis* through flagellin perception. *Nature*, 428(6984), 764-767.

SUPPLEMENTARY INFORMATION

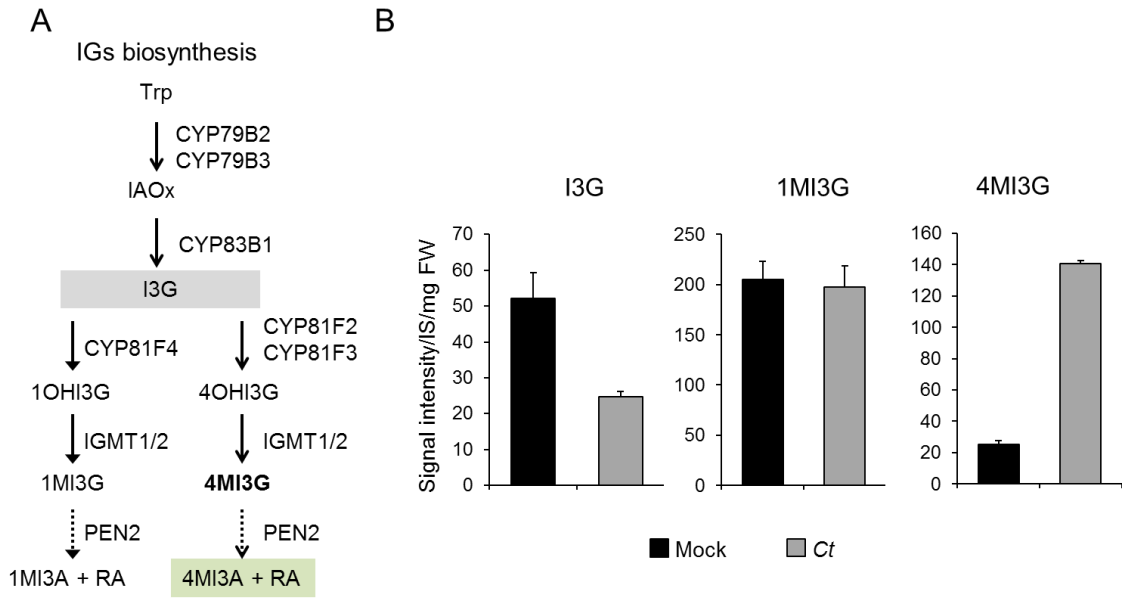

Supplementary Figure 1. 4MI3G production is induced during *Ct* colonization.

(A) A scheme for IG biosynthesis in Arabidopsis.

(B) Accumulation of I3G, 1MI3G and 4MI3G in roots at 3 days after *Ct* inoculation in 7 days-old WT plants. Metabolites contents were determined with liquid chromatography/mass spectrometry (LC/MS). 3 biological replicates for each sample. Error bars indicate standard errors. This experiment was conducted by Shigetaka Yasuda.

Supplementary Table 1. *CSEP* genes highly induced during *Ct* colonization in *cyp79B2 cyp79B3* plants.

		FPKM			
		1 dpi		3 dpi	
CSEP	Gene ID	WT	*cyp79B2 cyp79B3*	WT	*cyp79B2 cyp79B3*
CSEP1	CT04_00229	106.395	1054.75	216.565	858.209
CSEP2	CT04_01302	0	350.139	0	0
CSEP3	CT04_01355	0	279.579	0	0
CSEP4	CT04_02592	0	73.871	0	460.086
CSEP5	CT04_07149	0	311.892	0	152.486
CSEP6	CT04_08933	0	128.424	0	0
CSEP7	CT04_10528	0	457.223	0	0
CSEP8	CT04_10683	61.1864	3218.14	0	0
CSEP9	CT04_11124	16.3921	105.525	0	0
CSEP10	CT04_11158	0	0	553.919	1523.78
CSEP11	CT04_11194	0	0	24.9601	96.1132

Total of predicted *Ct* CSEPs = 133

Transcriptome analysis was conducted by Kei Hiruma.

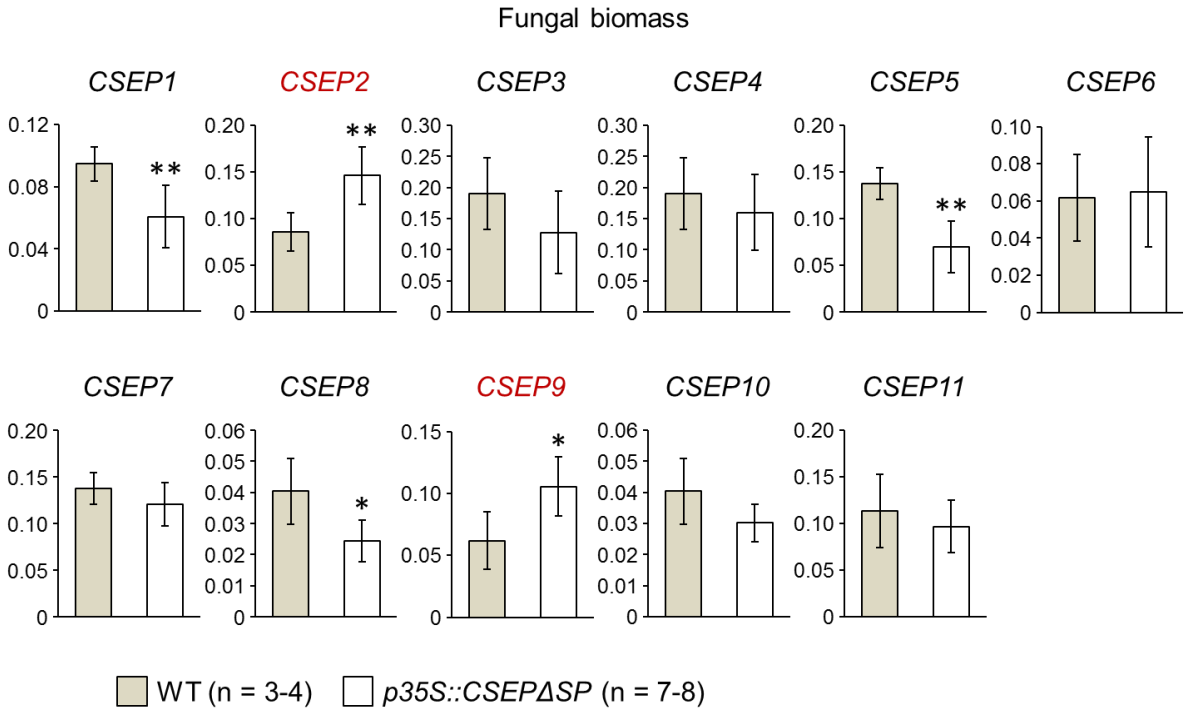

Supplementary Figure 2. Two *CSEPs* contribute to *Ct* root colonization.

qRT-PCR analysis for *Ct* biomass in 7 days-old WT and *pro35S::CSEPΔSP* transgenic plants (T2 generation) at 3 dpi with *Ct*. Error bars indicate standard errors. Asterisks indicate significant differences in the means between WT and *CSEP* transgenic plants (Two-tailed t-test, $p^* < 0.05$, $p^{**} < 0.001$). This experiment was conducted by Tsurukawa (Tsurukawa, 2020 Master thesis).

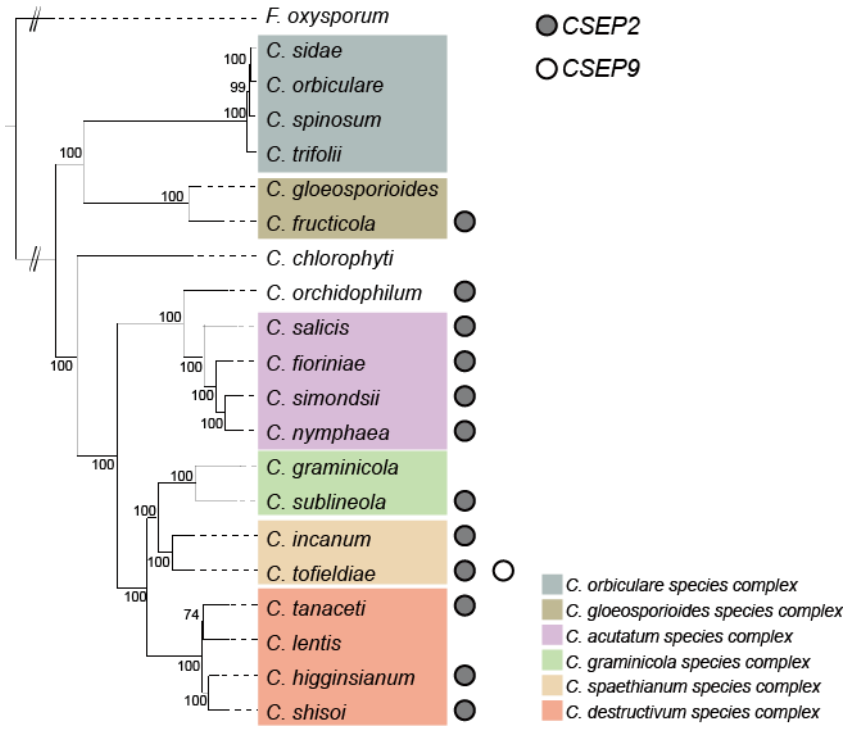

Supplementary Figure 3. Orthologs of two *CSEPs* in selected *Colletotrichum* species.
In a phylogenetic tree of *Colletotrichum* species (Gan et al., 2019), the presence of *CSEP2* and *CSEP9* orthologs is indicated by the colored circles on the right. Gray circle, *CSEP2*. White circle, *CSEP9*.